RESEARCH
ENGINEERING
PRODUCTION

AXISYMMETRIC LAMINAR

AND TURBULENT JETS OF HYDROGEN

WITH SIMPLE CHEMISTRY

By Harold Rosenbaum

Technical Report No. 331

N65-32088

January 4, 1963

GENERAL APPLIED SCIENCE LABORATORIES, INC.
MERRICK and STEWART AVENUES, WESTBURY, L.I., N.Y. · (516) ED 3-6960

TECHNICAL REPORT NO. 331

AXISYMMETRIC LAMINAR AND TURBULENT

JETS OF HYDROGEN WITH SIMPLE CHEMISTRY

By Harold Rosenbaum

Prepared for

George C. Marshall Space Flight Center
Huntsville, Alabama
Under Contract No. NAS8-2686

Prepared by
Research Deaprtment
General Applied Science Laboratories, Inc.
Merrick and Stewart Avenues
Westbury, L.I., New York

January 4, 1963   Approved by: _____

                                                          Antonio Ferri
                                                          President

TABLE OF CONTENTS

LIST OF SYMBOLS

a   radius of jet

A_i constants appearing in Equation (29)

$\bar{c}_{p_i}$ constants appearing in Equation (20)

H   stagnation enthalpy

h   static enthalpy

h_i static enthalpy of species i

K μ for laminar flow; $\epsilon \rho$ for turbulent flow

n   constant = 0. 025

P   offset circular probability function

r   radial coordinate

T   static temperature

T_r constant appearing in Equation (20)

U   velocity ratio u/u_e

u   velocity component in x-direction

v   velocity component in r-direction

$\dot{w}_i$ volumetric rate of production of ith species

W   mean molecular weight of mixture

x   axial coordinate

X_i mole fraction of ith species

Y_i mass fraction of ith species

$\bar{Y}_i$ element mass fraction of ith element

Δ_i constants appearing in Equation (20)

ϵ eddy viscosity for compressible flow

$\bar{\epsilon}$ eddy viscosity for incompressible flow

ω_i constants appearing in Equation (29)

ρ density of mixture

Subscripts

f   radius at flame sheet

inc   incompressible values

ℓ laminar values

t   turbulent values

e   external flow

AXISYMMETRIC LAMINAR AND TURBULENT

JETS OF HYDROGEN WITH SIMPLE CHEMISTRY

By Harold Rosenbaum

SUMMARY

32088

The problem of a uniform axisymmetric jet of pure hydrogen issuing into

a parallel free stream of air is discussed. There are considered both laminar

and turbulent flows under the assumption that all Prandtl and Lewis numbers are

equal to unity, and that the limiting chemical behaviors of frozen and equilibrium

flow prevail; the flame sheet approximation is applied to the equilibrium model.

Calculations are performed along a point on a typical trajectory for missile

launch.

AuThoR

I. INTRODUCTION

During the launch of multistage vehicles it is sometimes necessary to discharge overboard hydrogen, or other fuels, from the upper stages. Since combustion of these gases with the surrounding airstream may occur in the neighborhood of the vehicle, localized convective heating and alterations of the forces and momenta on the vehicle may result. A series of studies of the phenomena involved in the ejection, mixing and combustion of gaseous fuels is being carried out.

The problem considered here is that of a uniform axisymmetric jet of pure hydrogen issuing into a uniform parallel free stream. Both turbulent and laminar flow models with unity Prandtl and Lewis numbers are treated. The flow field is shown schematically in Fig. 1.

The analysis presented here represents an extension of work performed by Libby (Ref. 1) and Kleinstein (Ref. 2). In Ref. 2 a laminar axisymmetric jet of pure hydrogen issuing into and reacting with a moving air stream was analyzed. In both analyses a linearization of a modified Oseen nature was employed together was a standard von Mises transformation. The equation for the velocity field in the transformed plan was then reduced to a heat flow equation whose solution is known. The chemical behavior of the jet flow and the dominating viscous phenomena either laminar or turbulent, then determine the inverse transformation to the physical plane.

In this study the laminar reacting jet is considered by coupling the chemical model used in Ref. 1 with the fluid mechanical model discussed above. The turbulent reacting jet is analyzed much as in Ref. 1, but with the form of the eddy viscosity given in Ref. 1 modified according to the model of the eddy viscosity suggested in

Reference 3; this model is presently believed to be more correct than that employed in Reference 1.

Two limiting chemical behaviors are studied: frozen and equilibrium flow. The equilibrium composition is approximated by a "flame sheet model" after Reference 1. Assumption of unity Prandtl and Lewis numbers allows an application of Crocco integrals to the solution of the energy and mass fraction conservation equations.

II.   ANALYSIS

The equations of motion describing laminar and turbulent jets are taken to be identical in form, with mean turbulent quantities replacing their laminar counterparts. Assuming all laminar and turbulent Prandtl numbers and Lewis numbers equal to unity the governing equations are:

Conservation of Momentum:

$$\rho u \frac{\partial u}{\partial x} + \rho v \frac{\partial v}{\partial r} = \frac{1}{r} \frac{\partial}{\partial r} \left[Kr \frac{\partial u}{\partial r} \right] \tag{1}$$

Conservation of Energy:

$$\rho u \frac{\partial H}{\partial x} + \rho v \frac{\partial H}{\partial r} = \frac{1}{r} \frac{\partial}{\partial r} \left[Kr \frac{\partial H}{\partial r} \right] \tag{2}$$

Global Conservation of Mass:

$$\frac{\partial}{\partial x} (\rho u) + \frac{1}{r} \frac{\partial}{\partial r} (\rho v r) = 0 \tag{3}$$

Conservation of Species:

$$\rho u \frac{\partial Y_i}{\partial x} + \rho v \frac{\partial Y_i}{\partial r} = \dot{w}_i + \frac{1}{r} \frac{\partial}{\partial r} \left[Kr \frac{\partial Y_i}{\partial r} \right] \tag{4}$$

where for laminar flow:

$$K = \mu = \text{laminar coefficient of viscosity} \tag{5}$$

and for turbulent flow

$$K = \epsilon \rho; \quad \epsilon = \text{eddy viscosity coefficient} \tag{6}$$

The initial and boundary conditions are:

$x = 0$; $0 \leq r < a$

$u = u_j$; $v = 0$; $\qquad H = H_j$; $\qquad Y_1 = Y_3 = Y_4 \equiv 0$; $Y_2 = 1$

$x = 0 \qquad r > a$

$u = u_e \qquad v = 0 \qquad\qquad H = H_e$; $\qquad Y_2 = Y_3 = 0$; $Y_1 = Y_{1e}$; $Y_4 = Y_{4e}$

$x \geq 0$

$$\lim_{r \to \infty} ; H = H_e; \quad u = u_e; \quad v = 0; \quad Y_2 = Y_3 = 0; \quad Y_1 = Y_{1e} ; \quad Y_4 = Y_{4e}$$

with regularity condition applied along the jet centerline, $r = 0$.

Introduce a stream function:

$$\rho u r = \rho_e u_e \Psi \Psi_r \tag{7}$$

$$- \rho v r = \rho_e u_e \Psi \Psi_r$$

and apply the von Mises transformation, i.e. transform from $x, r \to x, \Psi$; then

$$r^2 = \int_0^{\Psi} \frac{2\rho_e u_e}{\rho u} \Psi' d \Psi' \tag{8}$$

and equation (1) becomes without approximation

$$\frac{\partial u}{\partial x} = \frac{1}{u_e \Psi} \frac{\partial}{\partial \Psi} \left[\frac{K \rho r^2 u}{\rho_e^2 u_e \Psi^2} \frac{\Psi}{\partial \Psi} \frac{\partial u}{\partial \Psi} \right] \tag{9}$$

Laminar Flow

Following the modified Oseen approximation of Kleinstein (Ref. 2) for laminar flow, assume

$$\frac{K \rho u r^2}{\rho_e^2 u_e^2 \Psi^2} \equiv \frac{\mu \rho r^2 u}{\rho_e^2 u_e^2 \Psi^2} \cong f(x) \tag{10}$$

Employing this assumption and introducing the additional transformation,

$$\xi = \int_0^{x_\ell} \frac{f(x)}{\Psi_j} \, dx_\ell \tag{11}$$

Equation (9) becomes

$$\frac{\partial U}{\partial \xi} = \frac{\Psi_j}{\Psi} \frac{\partial}{\partial \Psi} \left[\Psi \cdot \frac{\partial U}{\partial \Psi} \right] \tag{12}$$

where:

$$\Psi_j = a \left(\frac{\rho_j u_j}{\rho_e u_e} \right)^{1/2} \quad ; \quad \text{and} \quad U = \frac{u}{u_e}$$

In the present report the approximation function $f(x)$ in Equation (11) is along the jet center line, then

$$f(x) \simeq \frac{\mu_c}{\rho_e u_e}$$

and the inverse of equation (11) becomes,[1]

$$\frac{x_\ell}{\Psi_j} = \int_0^{\xi} \frac{\rho_e u_e}{\mu_c} \, d\xi \tag{13}$$

Turbulent Flow

For turbulent flow Libby (Ref. 1) has shown:

$$\frac{K \rho r^2 u}{\rho_e^2 u_e^2 \Psi^2} \equiv \frac{\epsilon \rho^2 r^2 u}{\rho_e^2 u_e^2 \Psi^2} \cong F(x)$$

and has approximated $F(x)$ by,

$$F(x) = \frac{\rho_0 \bar{\epsilon}}{\rho_e u_e}$$

---

(1) In Ref. (2) μ_c is taken to be a constant equal to μ_j. At the suggestion of G. Kleinstein it was decided here to take μ_c as a function of x to be evaluated along the jet center line.

where ρ_o = some reference density

$\bar{\epsilon}$ = incompressible eddy viscosity

$$= n \, (r_{1/2})_{inc} \, u_e \, [1 - U_c]$$

and $(r_{1/2})_{inc}$ is the jet half radius in the incompressible plane.

It has been shown, however, by Ferri et al (Ref. 3) that a more accurate representation of $F(x)$ might be:

$$F(x) \equiv \frac{\epsilon \, \rho^2 r^2 u}{\rho_e^2 u_e^2 \Psi^2} \cong \frac{n \, r_{1/2}}{\rho_e u_e} \quad [\rho_e u_e - \rho_c u_c] \tag{14}$$

where now $r_{1/2}$, the half radius in the compressible plane is defined by,

$$(\rho u)_{r_{1/2}} = \frac{1}{2} [\rho_e u_e + \rho_c u_c] \tag{15}$$

Employing the approximation (14) and the additional transformation:

$$\xi = \int_o^{x_t} \frac{F(x)}{\Psi_j} \, dx_t$$

Equation (9) transforms to:

$$\frac{\partial U}{\partial \xi} = \frac{\Psi_j}{\Psi} \frac{\partial}{\partial \Psi} \left[\Psi \frac{\partial U}{\partial \Psi} \right] \tag{16}$$

The inverse transformation for the axial coordinate is

$$\frac{x_t}{\Psi_j} = \int_o^{\xi} \frac{1}{F(x)} \, d\xi \tag{17}$$

The equations describing the velocity field, equations (12) and (16), for laminar and turbulent flow respectively, are identical in form and independent of the density and viscosity. The initial and boundary conditions for both cases corresponding to the flow field shown in Fig. 1 are as follows:

$$U(0, \Psi) = U_j = u_j/u_e \quad ; \quad 0 \le \Psi_j < \Psi$$

$$\lim_{\Psi \to \infty} U(\xi, \Psi) = 1$$

with the regularity conditions applied along the jet center line, $\Psi = 0$. The solution of either equation, 12 or 16, subject to the above condition is well known in the theory of heat conduction (cf Ref. 1 and 2); it is:

$$P = \frac{1-U}{1-U_j} = \frac{\Psi_j}{2\xi} e^{-\left(\frac{\Psi}{\Psi_j}\right)^2 \frac{\Psi\xi}{\Psi_j}} \int_0^1 e^{-\Psi'^2 \frac{\Psi}{\xi}/\Psi_j} I_0\left[\Psi'\left(\frac{\Psi}{\Psi_j}\right)\left(\frac{2\xi}{\Psi_j}\right)^{-1}\right] \Psi' \, d\Psi'$$

(18)

where P is the offset circular probability function and has been tabulated by Masters (Ref. 4).

Transformation to Physical Coordinates - General Remarks

To apply the solution given by equation (18) the inverse of the transformations given by equation (8), and by either equation (13) or equation (17) must be employed. Therefore it is necessary to consider the chemical model to obtain the density ratio ρ/ρ_e and the center line properties needed to perform these transformations. The chemical model employed here and the resulting solutions for the density ratio follows that of Libby (Ref. 2), i.e. the jet is assumed to be of pure gaseous hydrogen and the external stream to be air. Moreover, there is considered

a mixture of four species, denoted by the subscripts i = 1, 2, 3, 4, respectively, molecular oxygen, molecular hydrogen, water and nitrogen. The two limiting chemical cases of frozen and equilibrium flow are discussed. Moreover, a "flame sheet model" is used to replace the equilibrium condition and nitrogen is considered to occur as an inert diluent only.

Inspection of equations (1) and (2) and the boundary and initial conditions leads to a Crocco integral relation for the stagnation enthalpy;

$$H = \frac{[\, H_e(U-U_j) + H_j (1-U) \,]}{(1-U_j)} \equiv \frac{u_e{}^2}{2} + h \tag{19}$$

It is advantageous to employ an analytical representation for the static species enthalpy $h_i = h_i (T)$. Assume therefore,

$$h_i \cong \Delta_i + \bar{c}_{p_i} (T-T_r) \tag{20}$$

where Δ_i, $\bar{c}_{p_i}$, T_r are constants selected to represent h_i in the temperature range desired. Equations (19) and (20) then yield the temperature T.

Frozen Flow

For frozen flow $\dot{w}_i$ and $Y_3 \equiv 0$; thus injection of equations (1) and (4) lead to Crocco integral relations of the form

$$Y_1 = Y_{1e} (U - U_j) \Big/ (1-U_j)$$

$$Y_2 = (1-U) \Big/ (1-U_j)$$

$$Y_3 \equiv 0$$

$$Y_4 = Y_{4e} (U - U_j) \Big/ (1-U_j)$$

(21)

Equilibrium Flow

Since there can be no net production of atoms in a reacting gas it is advantageous to introduce the element mass fraction, (cf; e.g., Ref. 1)

$$\widetilde{Y}_1 = Y_1 + \frac{W_1}{2W_3} Y_3$$

$$\widetilde{Y}_2 = Y_2 + \left(W_2/W_3\right) Y_3$$

$$\widetilde{Y}_4 = Y_4$$

(22)

Substitution of equation (22) into equation (4) yields:

$$\frac{\rho u \partial \widetilde{Y}_i}{\partial x} + \frac{\rho v \partial \widetilde{Y}_i}{\partial r} = \frac{1}{r} \frac{\partial}{\partial r} \left[K r \frac{\partial \widetilde{Y}_i}{\partial r} \right]$$

(23)

$$i = 1, 2, 4$$

Once again consideration of these equations and of the initial and boundary

conditions lead to Crocco relations of the form:

$$\tilde{Y_1} = Y_{1e} (U-U_j) \Big/ (1-U_j)$$

$$\tilde{Y_2} = (1-U) \Big/ (1-U_j)$$

$$\tilde{Y_4} = Y_4 = Y_{4e} (U-U_j) \Big/ (1-U_j)$$

(24)

where the additional equation for the determination of the species Y_i is obtained

from the equilibrium condition. Since the equilibrium constant is large for the

temperatures of interest here, Libby (Ref. 1), suggests a flame sheet model

approximation. It is assumed that, for $U_j < 1$ for example, $Y_1 \equiv 0$ when

$U_j \leq U < U_f$ and $Y_2 = 0$ when $U_f < U$, where U_f is defined such that $Y_1 = Y_2 \equiv 0$.

Therefore:

$$U_f = \left[1 + \frac{2W_2 Y_{1e}}{W_1} U_j \right] \Big/ \left[1 + \frac{2W_2 Y_{1e}}{W_1} \right]$$

(25)

Once the concentrations have been determined, equations (19) and (20) may be

solved for the temperature by employing the definition;

$$h = \sum_{i=1}^{4} Y_i h_i$$

hence:

$$T - T_r = \frac{\left[H_e (U-U_j) + H_j (1-U) \right] (1-U_j)^{-1} - \frac{u_e^2}{2} U^2 - \Sigma Y_i |\Delta_i|}{\Sigma Y_i c_{p_i}}$$

(26)

Use of the equation of state:

$$p = \rho \, RT \sum \frac{Y_i}{w_i}$$

allows determination of the density ratio;

$$\frac{\rho_e}{\rho} = \left(\frac{T}{T_e}\right)\left(\frac{W_e}{W}\right) \tag{27}$$

Determination of Center Line Viscosity

In order to perform the transformation corresponding to equation (13), the viscosity along the jet center line, μ_c, of the gas mixture must be calculated. Following Bromley (Ref. 5) write

$$\mu_m = \sum_{i=1}^{n} \frac{\mu_i}{1 + \frac{1}{X_i} \sum_{\substack{j=1 \\ j \neq i}}^{n} X_j \, \Phi_{ij}} \tag{28}$$

where Φ_{ij} is given by,

$$\Phi_{ij} = \left[1 + \left(\frac{\mu_i}{\mu_j}\right)^{1/2} \left(\frac{W_j}{W_i}\right)^{1/4} \right]^2 \Bigg/ \frac{4}{\sqrt{2}} \left[1 + \frac{W_i}{W_j} \right]^{1/2} \tag{29}$$

and X_i = mole fraction = $\dfrac{W}{W_i} Y_i$

A description for the viscosity of the individual species μ_i was assumed in the form,

$$\mu_i = A_i \, (T)^{\omega_i} \tag{30}$$

where A_i and ω_i are constants such that Equation (30) represents μ_i in the temperature range desired.

All of the dependent flow variables have now been determined as functions of the transformed variables Ψ, ξ. Numerical integration of equation (8) and of either equation (13) or equation (17) is now possible to relate the dependent variables to the physical coordinates x and r.

Of particular interest here are the values of the dependent variables along the jet center line and the length of the flame sheet; i. e., the axial location (denoted by x_{f_ℓ} and x_{f_t} for laminar and turbulent flow respectively) of the interaction of the flame sheet and the jet center line. This point is defined by the condition

$$U(0, \xi) = U_f$$

Calculations

As an example of the foregoing analysis, calculations were performed for conditions appropriate to those found to yield minimum reaction lengths and thus to be critical on a typical launch trajectory in (Ref. 6). Following are the particular values of jet and gas parameters considered:

$H_e=$	365.3 cal/gm		$A_2 =$	$.208 \times 10^{-6}$ lb/ft sec
$u_e^2/2=$	370.5 cal/gm		$A_3 =$	$.833 \times 10^{-7}$ "
$\delta_e=$	1.295×10^{-5} lb/ft^3		$A_4 =$	$.305 \times 10^{-6}$ "
$T_e=$	275.75 °K		$\omega_2 =$	0.6
$\delta_j =$	7.926×10^{-6} lb/ft^3		$\omega_3 =$	0.8
$a =$	1 inch		$\omega_4 =$	0.65
$\bar{c}_{p_1}$	.26403	cal/gm°K	$W_1 =$	32
$\bar{c}_{p_2}$	.3654	"	$W_2 =$	2
$\bar{c}_{p_3}$	.56361	"	$W_3 =$	18
$\bar{c}_{p4}$	.28382	"	$W_4 =$	28
$\Delta_1 =$	185.23	"	$T_r =$	997.71°K
$\Delta_2 =$	2687.9	"	$Y_{1e}=$	0.232
$\Delta_3 =$	2881.3	"	$Y_{4e} =$	0.768
$\Delta_4 =$	200.05	"	$n =$	0.025

For a jet temperature of $T_j = 265°K$, three values of the velocity ratio U_j (0.33, 0.5, 0.8) were chosen. A jet temperature of $T_j = 60°K$ and velocity ratio of $U_j = 0.5$ was also considered. Figures 2 - 5 show the flame sheets obtained from the model for both laminar and turbulent equilibrium flow for the flight and gas conditions cited above. Figures 6 - 25 show the distribution of temperature, species concentrations and velocities along the jet center line from the jet to the point of intersection of the flame sheet and the jet center line. Figures 26 - 37 show the variation of the temperature ratio and the concentration of O_2, H_2O and H_2 along the center line far from the jet.

It is of interest to note that for a given set of flight conditions, there appears to be a dimensionless flame length that is virtually independent of the jet velocity ratio U_j, within the range of calculations performed here. For laminar flow this ratio appears as:

$$\frac{x_{f,\ell}}{a\left(\frac{\rho_j u_j \, a}{\mu_j}\right)} \cong \text{constant} = c_1$$

Therefore, for laminar flow, the length of the flame sheet is proportional to the square of the jet radius (a^2) and to the first power of the jet mass flow ($\rho_j u_j$).

For turbulent flow this ratio appears as:

$$\frac{x_{f,t}}{a\left(\frac{\rho_j u_j}{\rho_e u_e}\right)^{1/2}} \simeq \text{constant} = c_2$$

Hence the turbulent flame length varies as the first power of the jet radius (a) and

the square root of the mass flow ratio ($\rho_j u_j / \rho_e u_e$). It can be seen that the ratio of

laminar to turbulent flame lengths is approximately:

$$\frac{x_{f,\ell}}{x_{f,t}} \cong \frac{\dfrac{a\,\rho_j u_j}{\mu_j}}{\dfrac{\rho_j u_j}{\rho_e u_e}}_{1\ 2}\ \frac{c_1}{c_2} \cong 10^2$$

for the range of conditions studied here.

CONCLUSIONS

The properties of a uniform axisymmetric jet of pure hydrogen issuing into a uniform parallel free stream has been presented for both laminar and turbulent flow with simplified transport properties and simplified chemistry. All Prandtl and Lewis numbers have been assumed equal to unity and the two limiting cases of chemical behavior, frozen and equilibrium, are considered.

Calculations are presented for a particular set of flight variables of interest in an existing launch vehicle. It is found for laminar flow, that the flame length varies as the square of the jet radius and the first power of the jet mass flux. For turbulent flow the flame length is proportional to the first power of the jet radius and to the 1/2 power of the mass flow ratio $\dfrac{\rho_j u_j}{\rho_e u_e}$. A comparison of the flame lengths encountered in laminar and turbulent flow, for conditions considered here, indicate a ratio of

$$\frac{x_{f, \ell}}{x_{f, t}} \cong 10^2$$

REFERENCES

1. Libby, P. A., Theoretical Analysis of Turbulent Mixing of Reactive Gases With Application to Supersonic Combustion of Hydrogen. American Rocket Society Journal, Vol. 32, No. 3, March 1962.

2. Kleinstein, G., An Approximate Solution for the Axisymmetric Jet of a Laminar Compressible Fluid. Polytechnic Institute of Brooklyn, ARL 51, April 1961.

3. Ferri, A., Libby, P. A., Zakkay, V., Theoretical and Experimental Investigation of Supersonic Combustion. ARL 62-467, Polytechnic Institute of Brooklyn, Sept. 1962.

4. Master, J. I., Some Applications in Physics of the P Function, Journal of Chemical Physics, October 1955, Vo. 23.

5. Bromley, L. A.; and Wilke, C. R., Viscosity Behavior of Gases, Industrial and Engineering Chemistry, Vol. 43, July 1951.

6. Libby, P. A., Pergament, H. S., Taub, P., Engineering Estimates of Flow Lengths Associated With The Combustion of Hydrogen-Air Mixtures During a Launch Trajectory, GASL Tech. Report TR-330, December 1962.

EDGE OF MIXING REGION
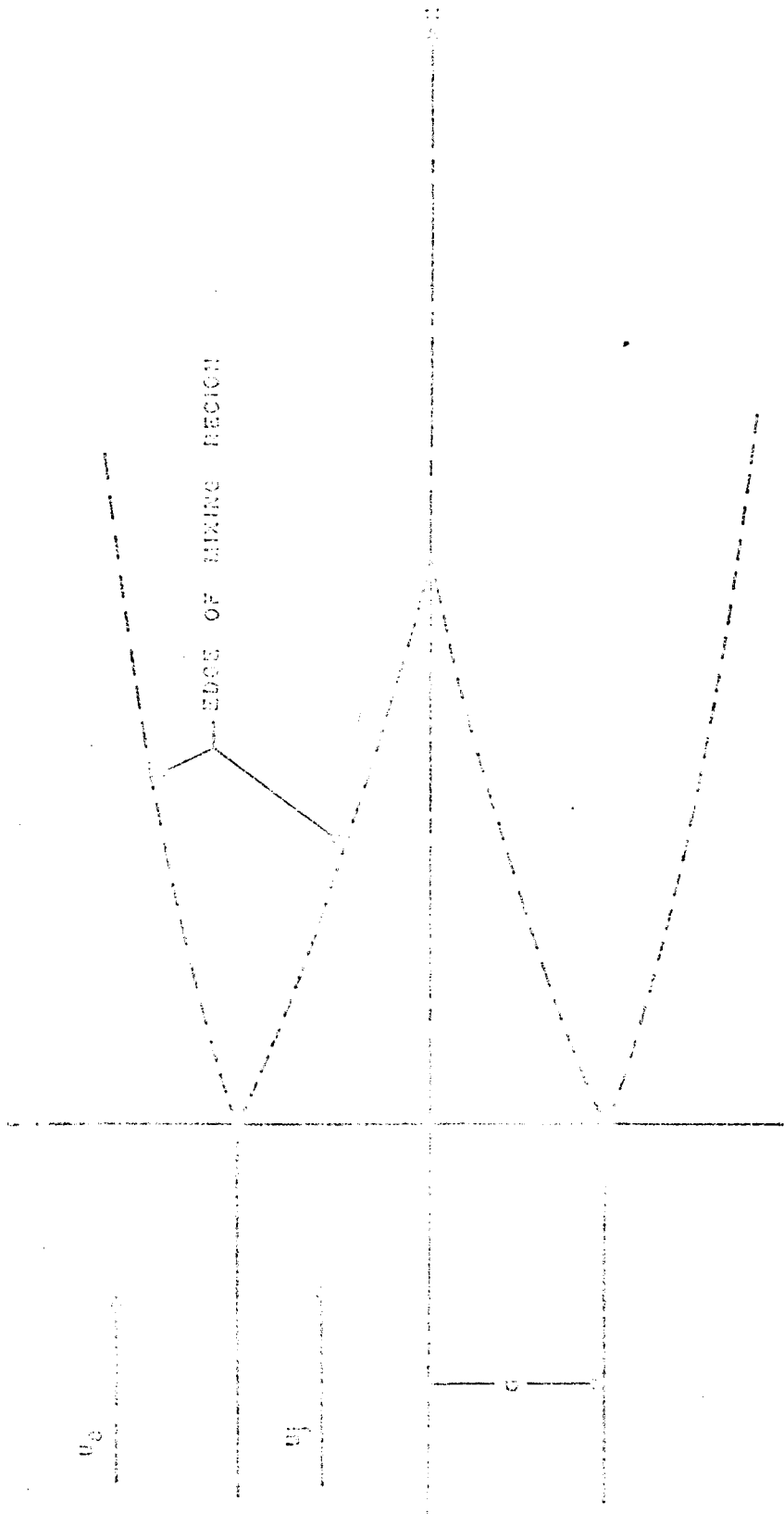
FIG. 1 SCHEMATIC OF FLOW REGION
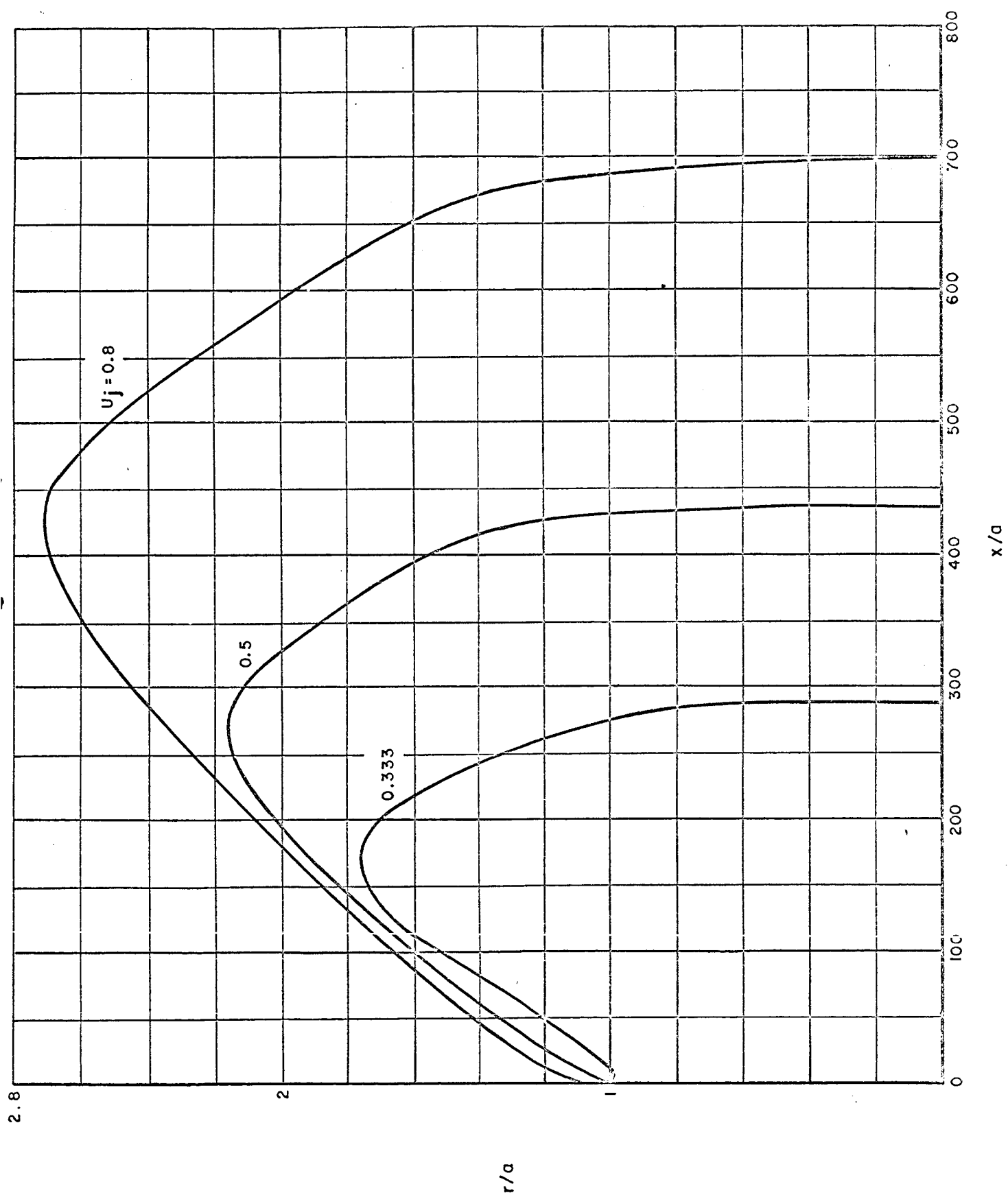
FIG. 2 LAMINAR FLAME SHEETS $T_j = 265°K$
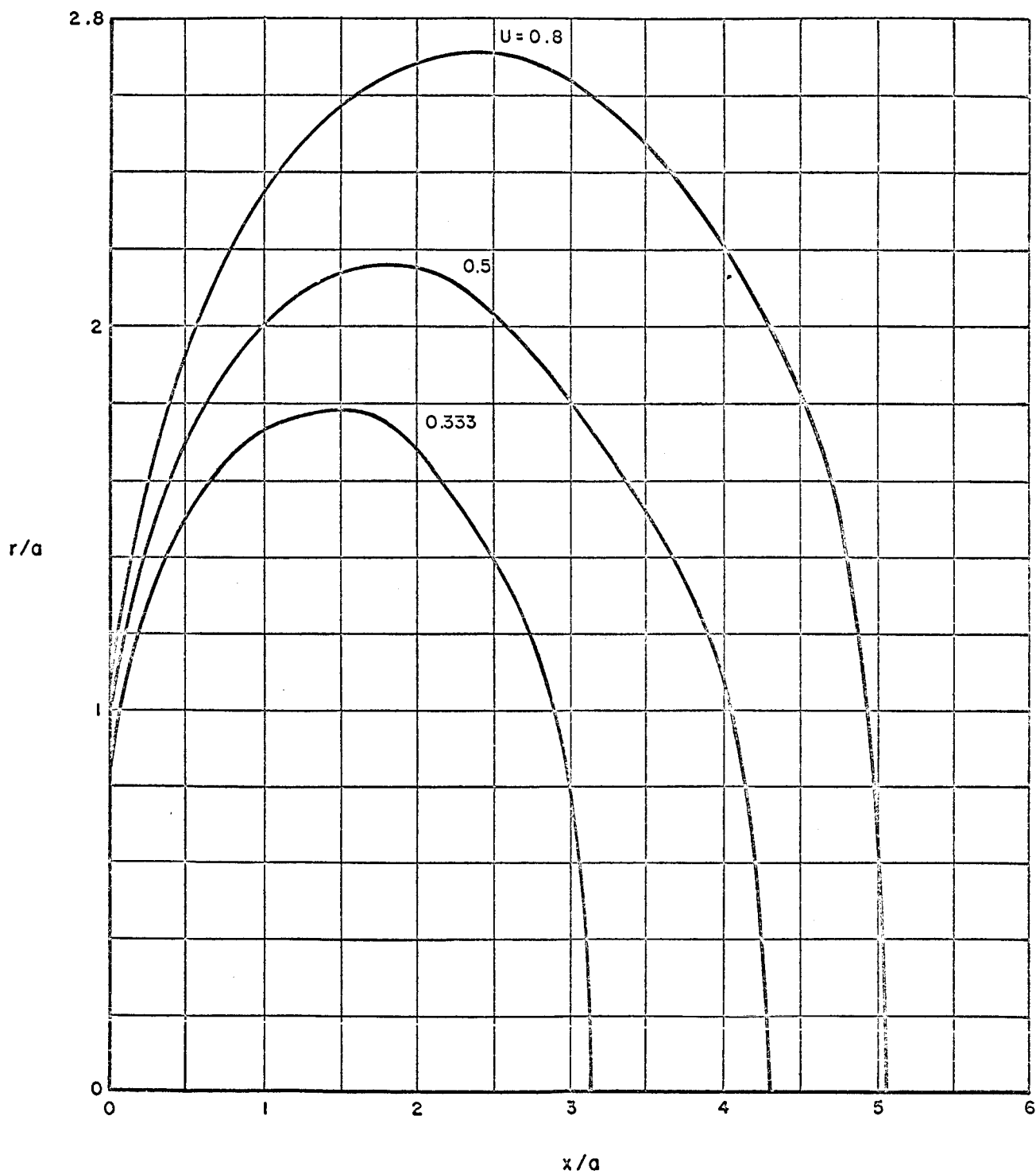
FIG. 3 TURBULENT FLAME SHEETS $T_j = 265°K$
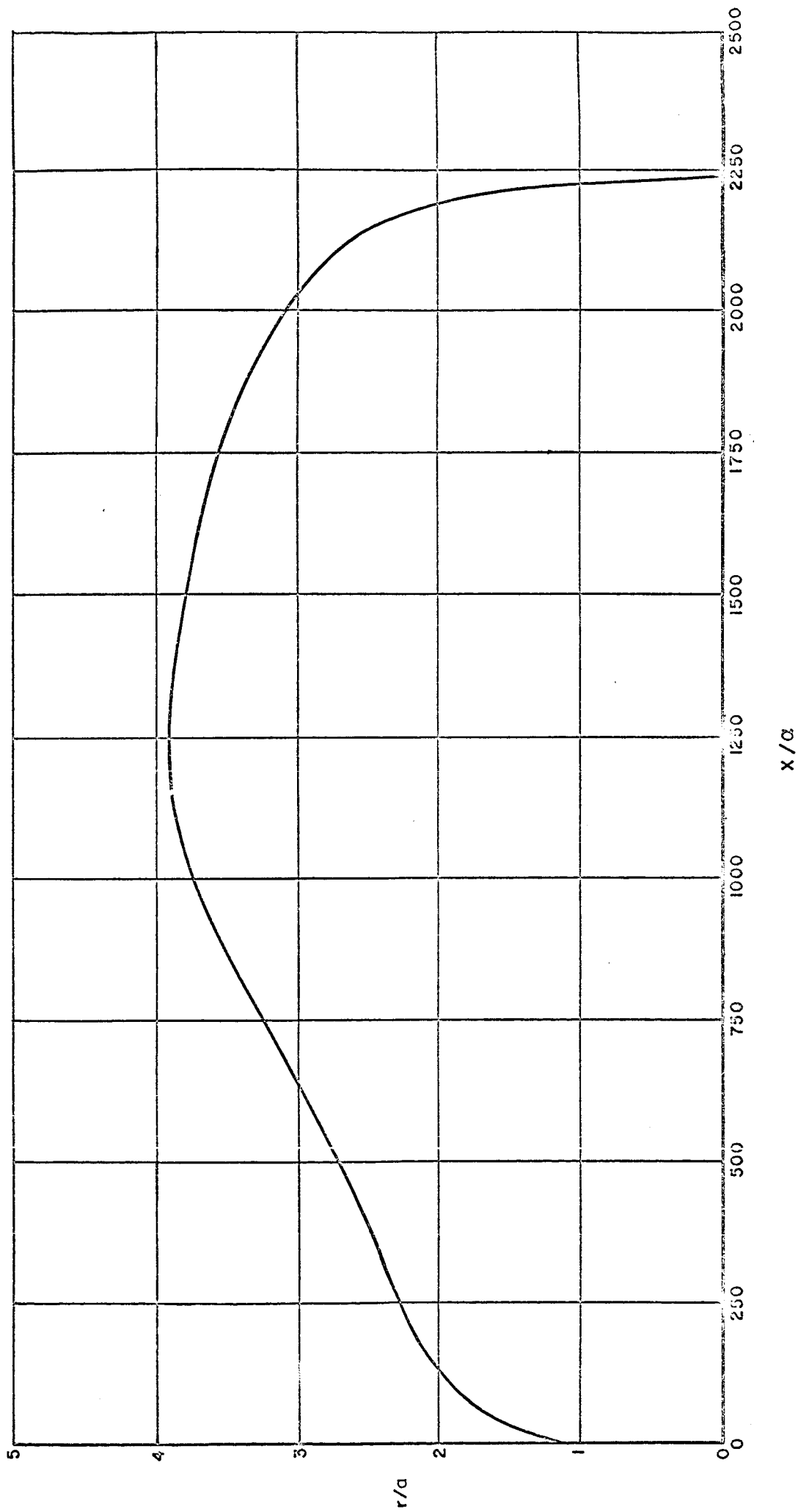
FIG. 4   LAMINAR JET $T_j = 60°K$
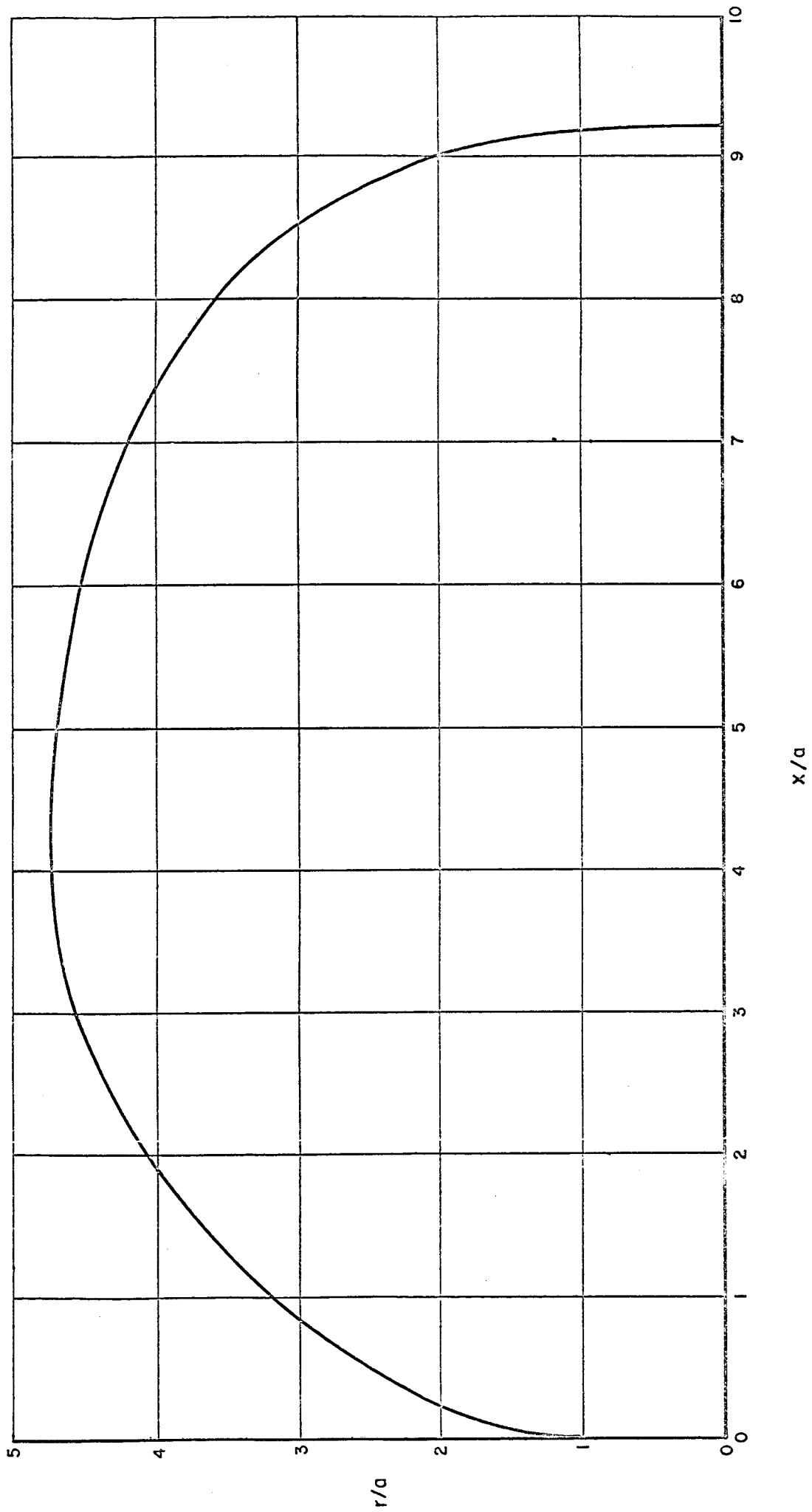
FIG. 5 TURBULENT FLAME SHEET - $T_j = 60°$ K

23

24
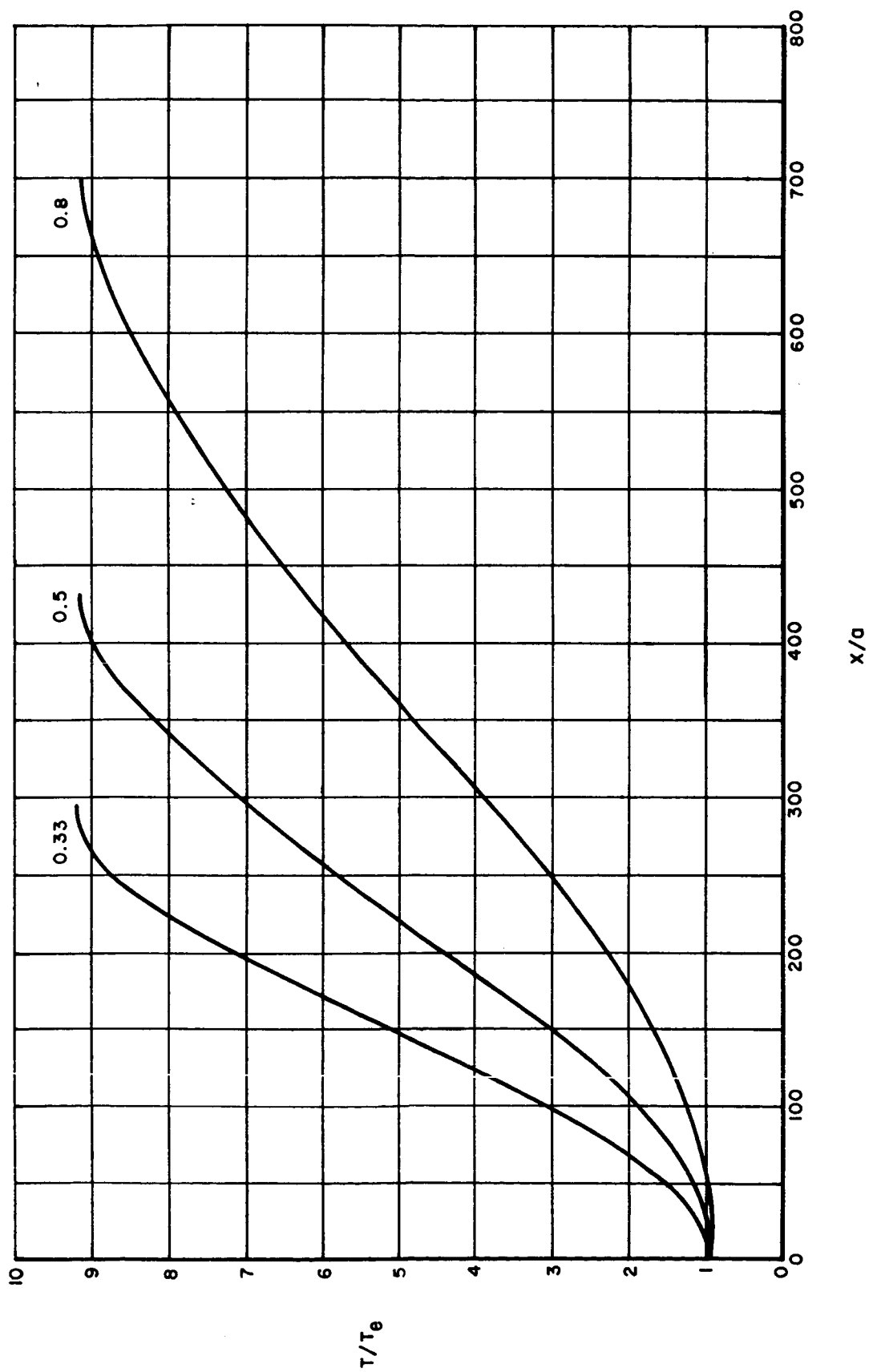
FIG. 6 TEMPERATURE DISTRIBUTION ALONG THE JET CENTER LINE LAMINAR — T_j = 265°K
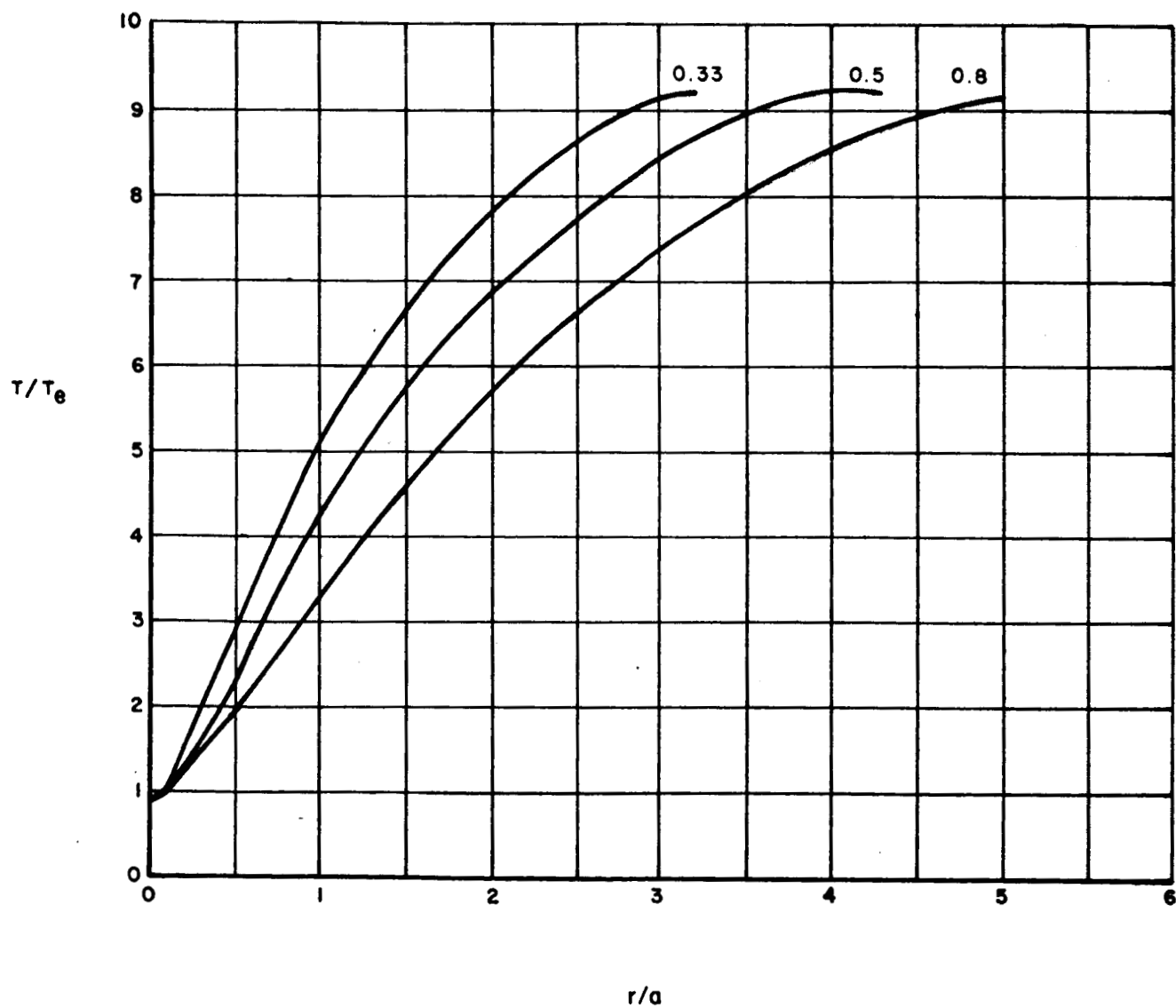
FIG. 7 TEMPERATURE DISTRIBUTION ALONG THE JET CENTER LINE TURBULENT
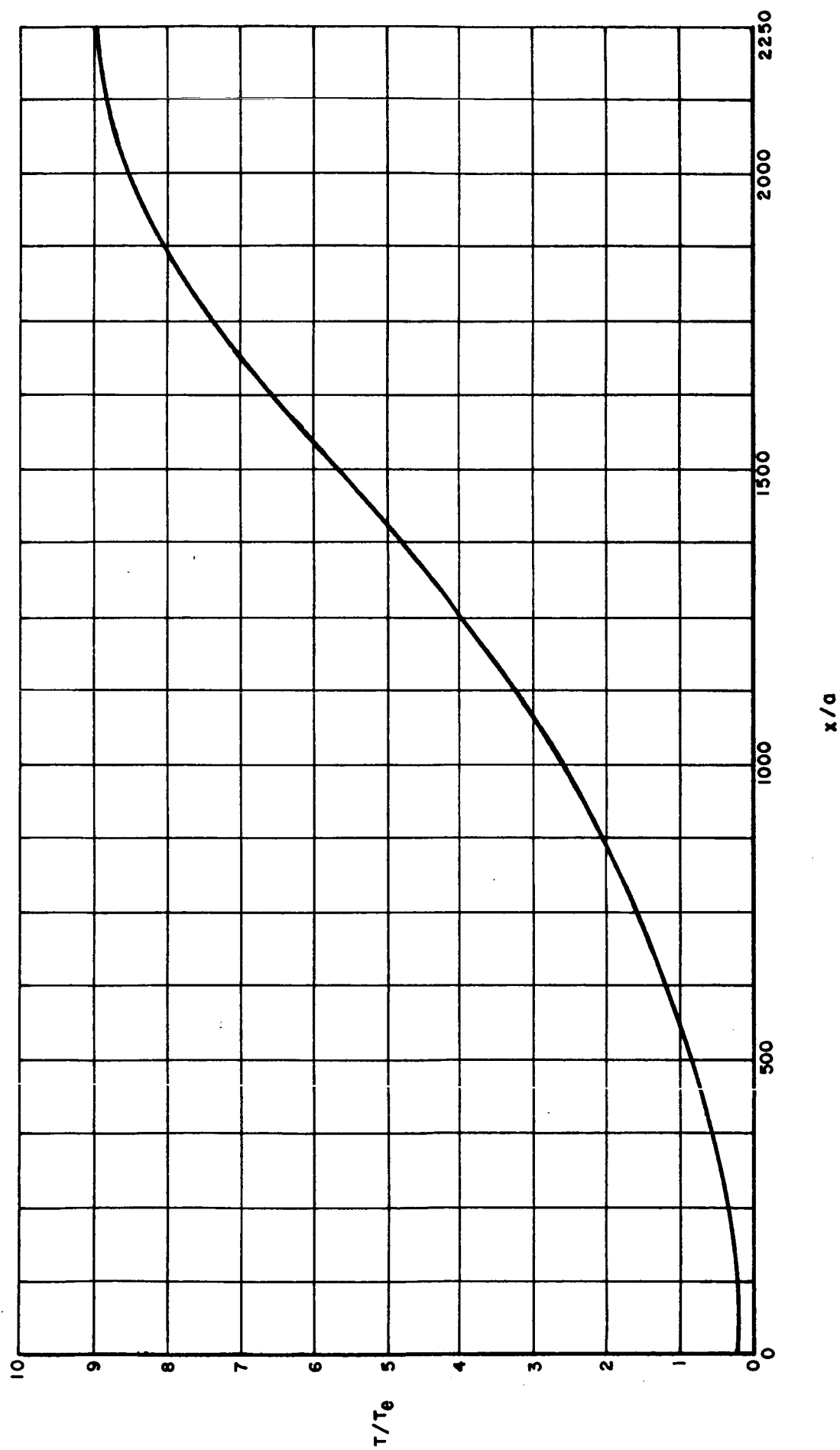
$T_j = 265° K$

FIG. 8 TEMPERATURE DISTRIBUTION ALONG THE JET CENTER LINE LAMINAR $T_j = 60°K$ $U_j = 0.5$
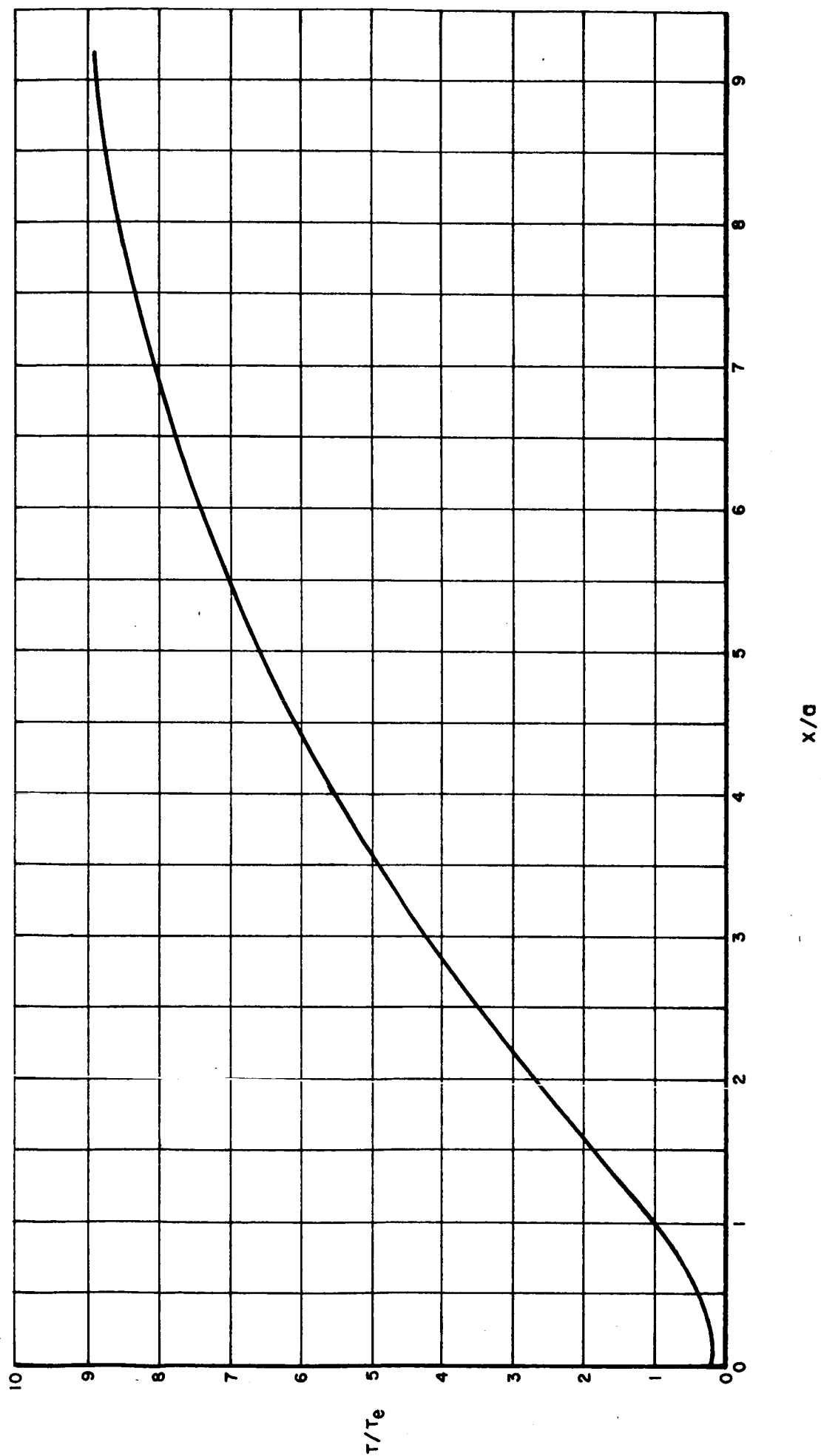
FIG. 9 TEMPERATURE DISTRIBUTION ALONG THE JET CENTER LINE - TURBULENT, U_j = .5 T_j = 60
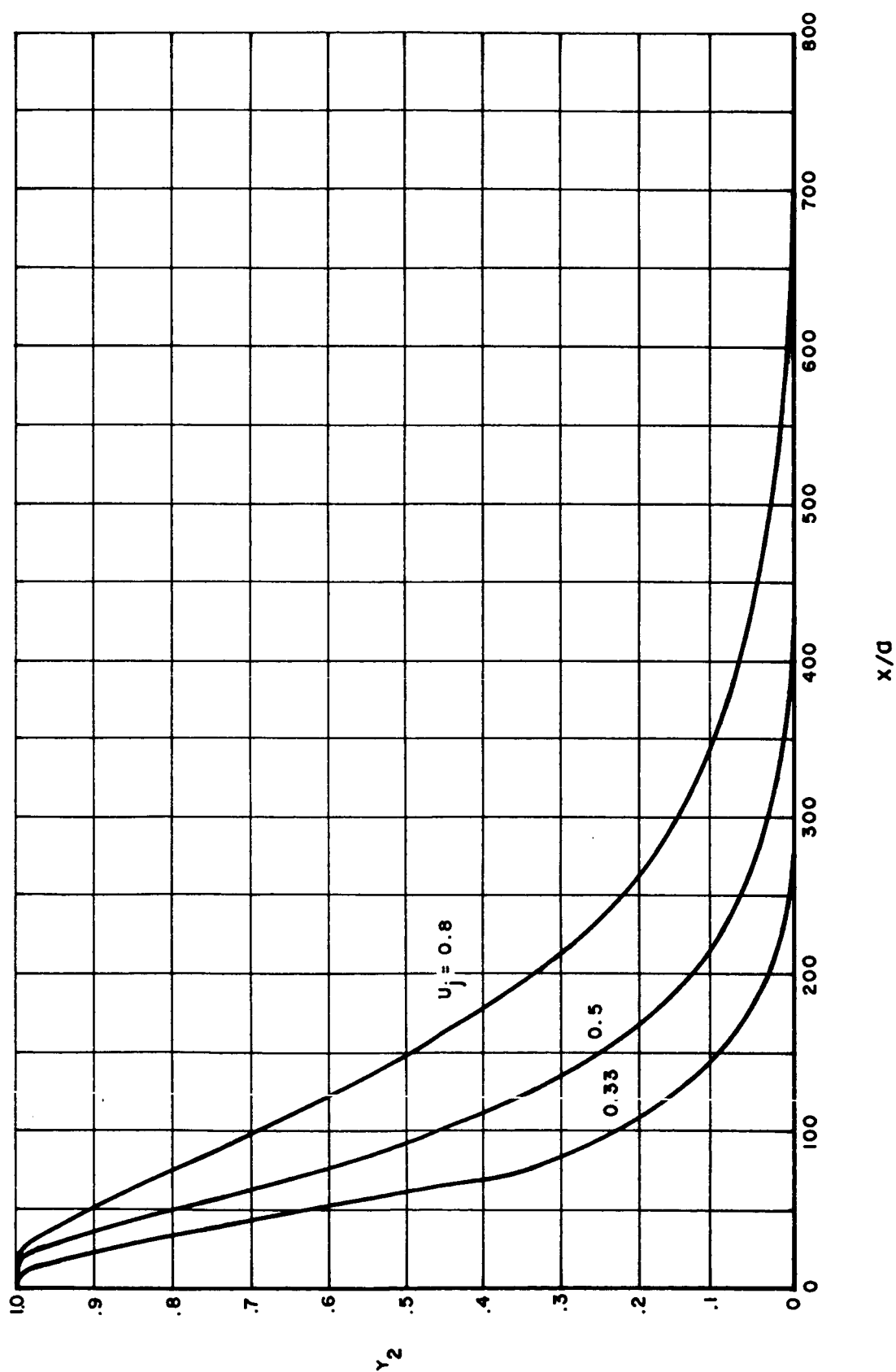
FIG. 10 DISTRIBUTION OF HYDROGEN ALONG THE JET CENTERLINE LAMINAR $T_j = 265\,°K$

$U_j = 0.8$

0.5

0.33
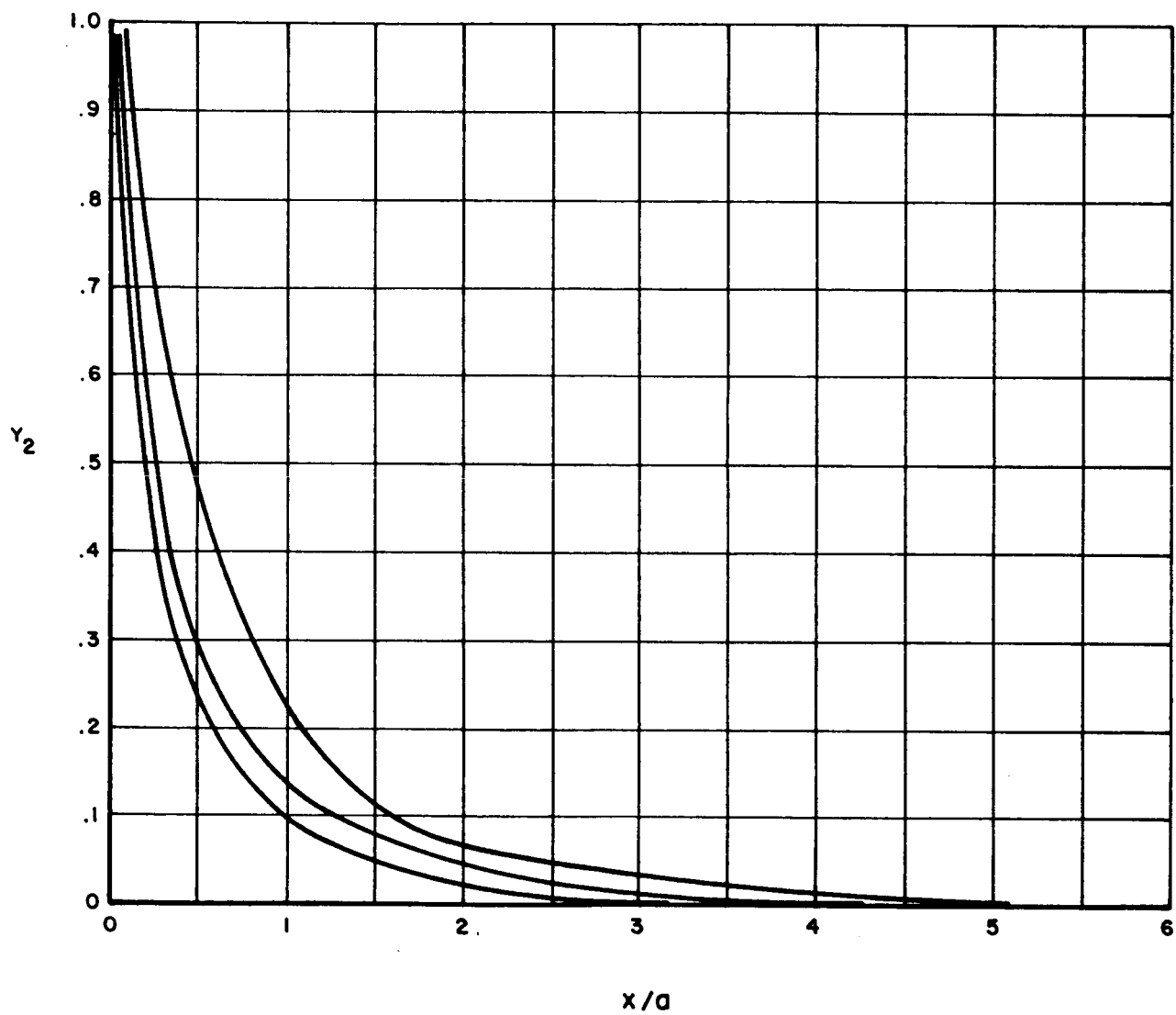
FIG. II DISTRIBUTION OF HYDROGEN ALONG THE JET CENTERLINE TURBULENT
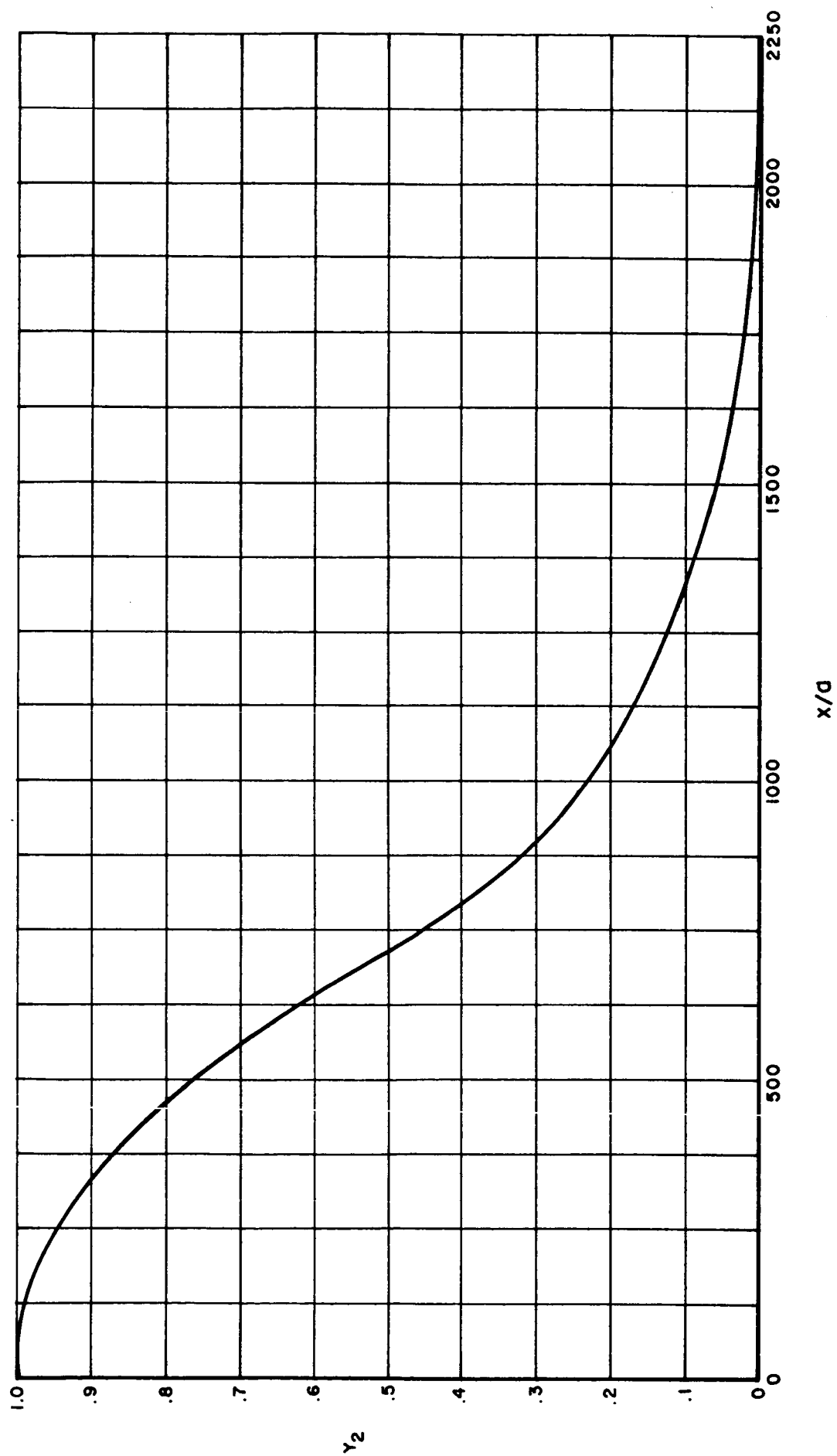
$T_j = 265 \,°K$

FIG. 12 DISTRIBUTION OF HYDROGEN ALONG THE JET CENTERLINE LAMINAR $T_j = 60$ °K
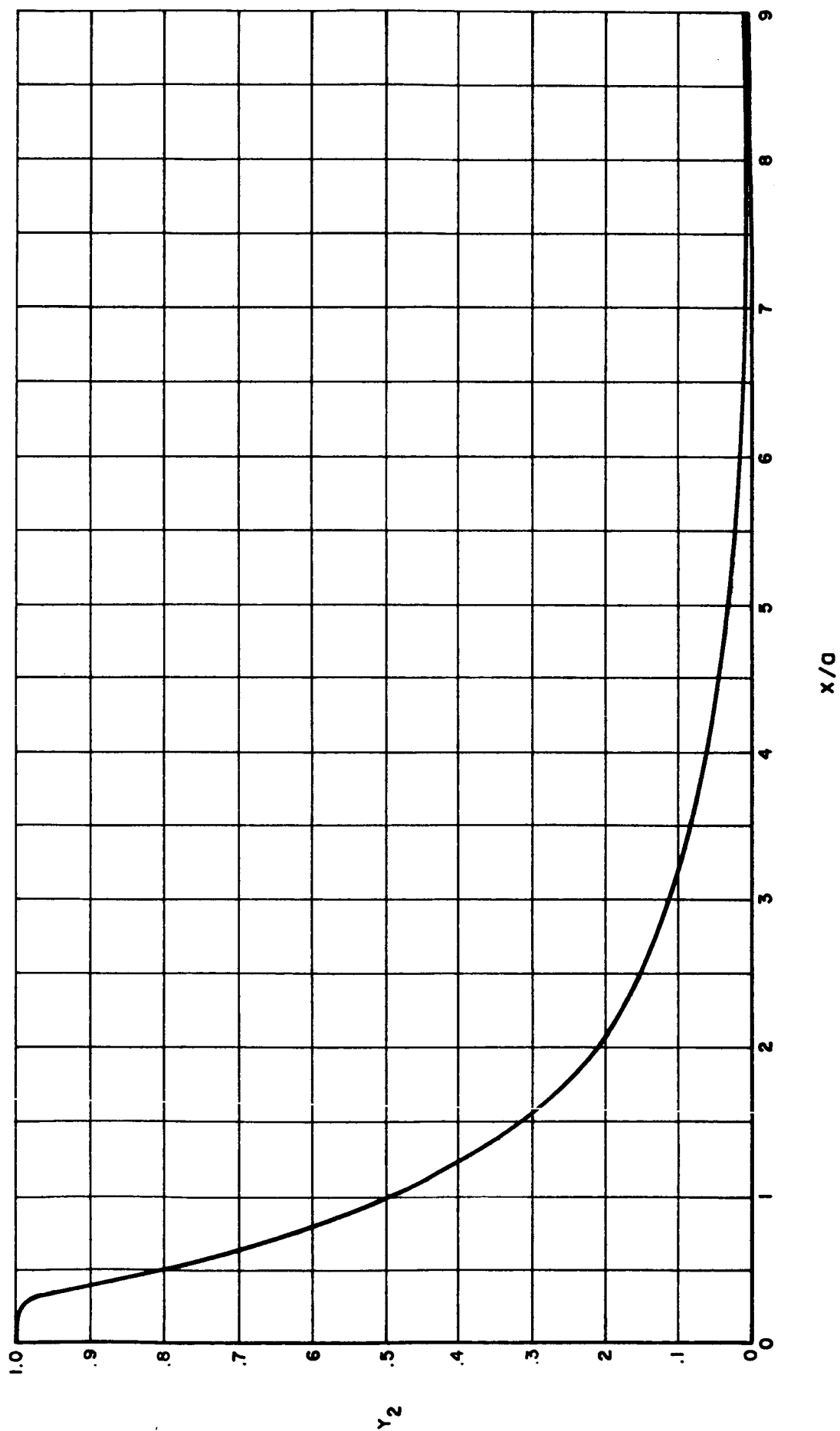
FIG. 13 DISTRIBUTION OF HYDROGEN ALONG THE JET CENTERLINE TURBULENT $T_j = 60 \, °K$
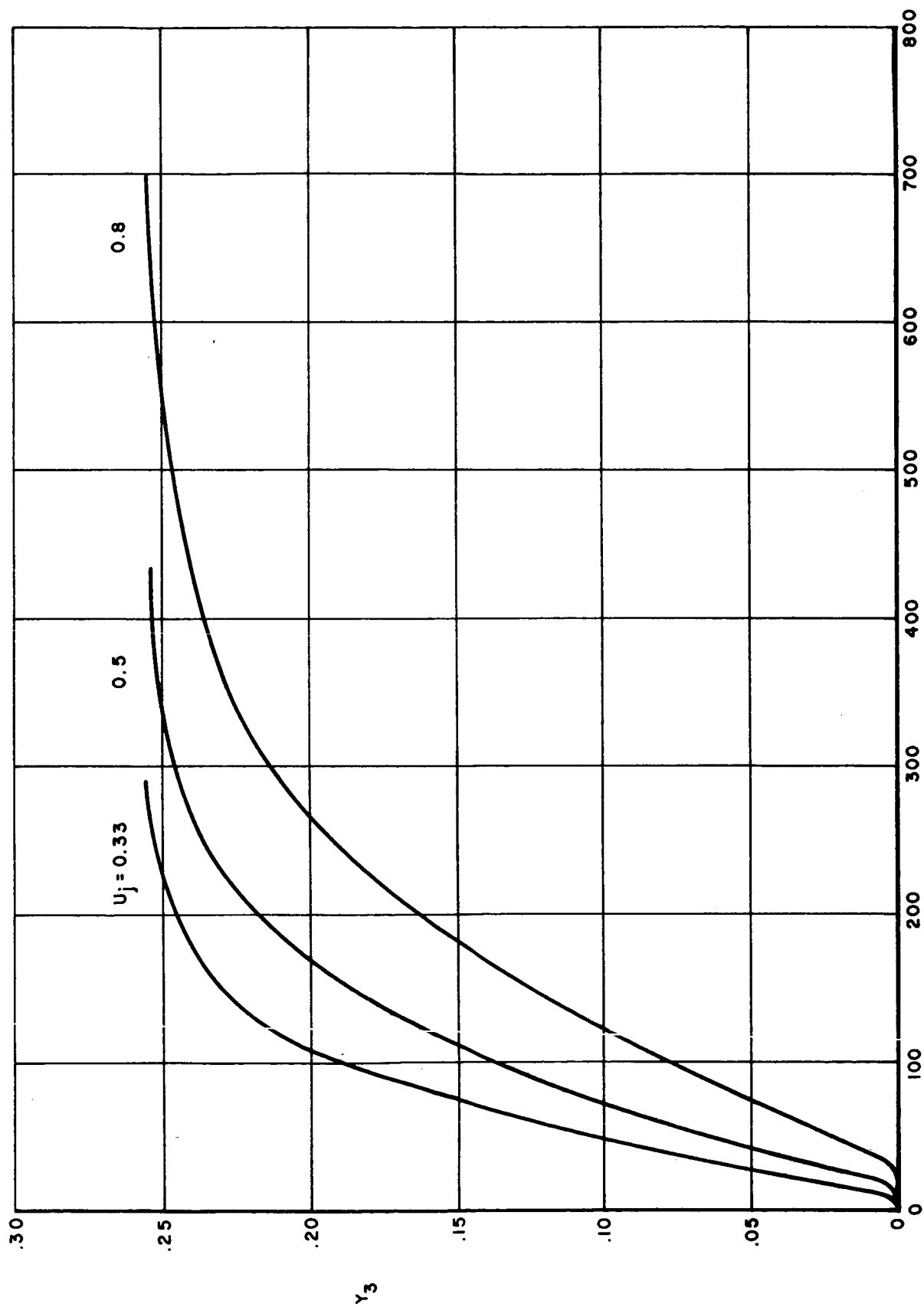
FIG. 14 DISTRIBUTION OF H_2O ALONG THE JET CENTERLINE LAMINAR $T_j = 265\,°K$
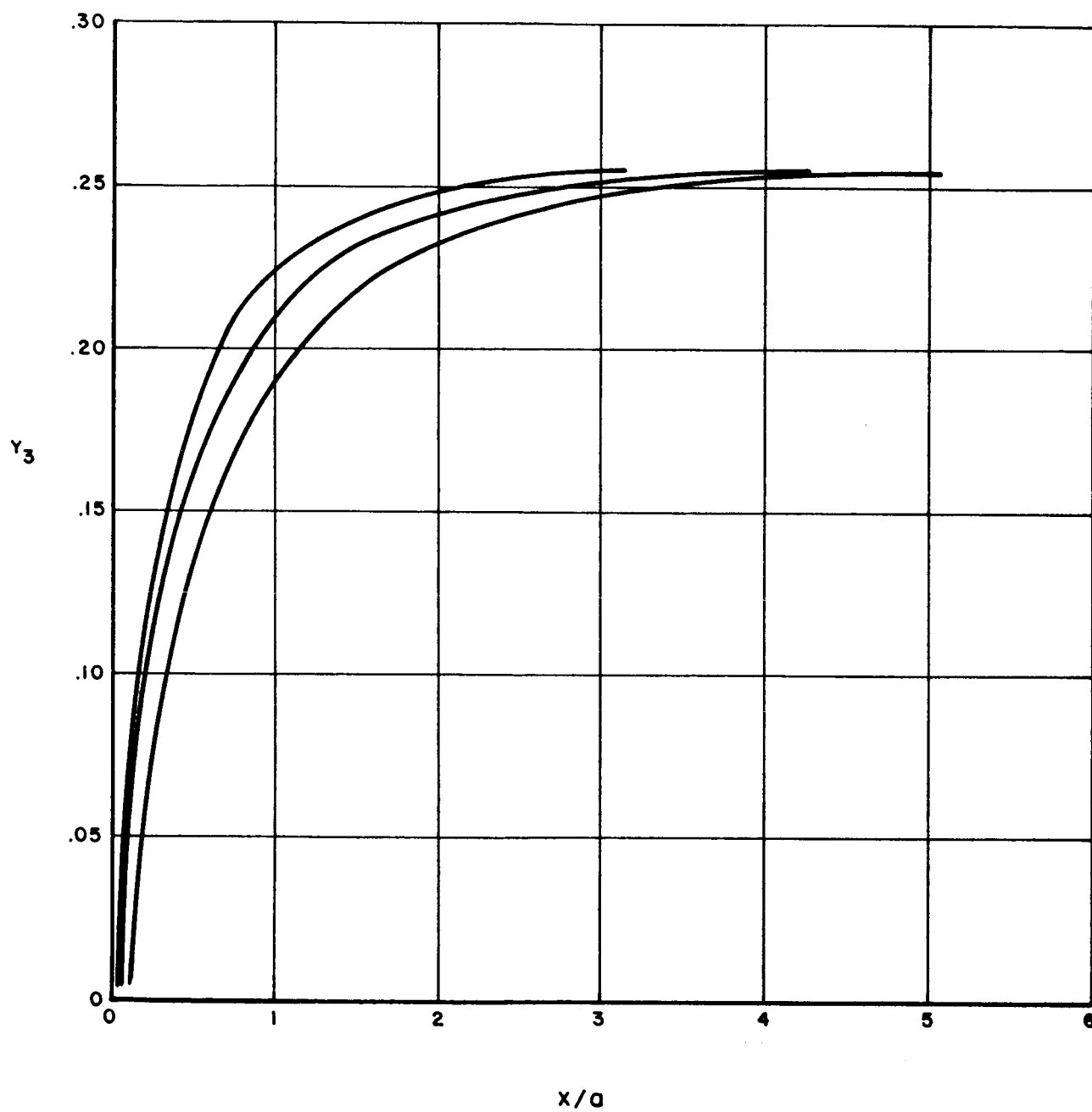
FIG. 15 DISTRIBUTION OF H_2O ALONG THE JET CENTERLINE TURBULENT
$T_j = 265 \ ^\circ K$
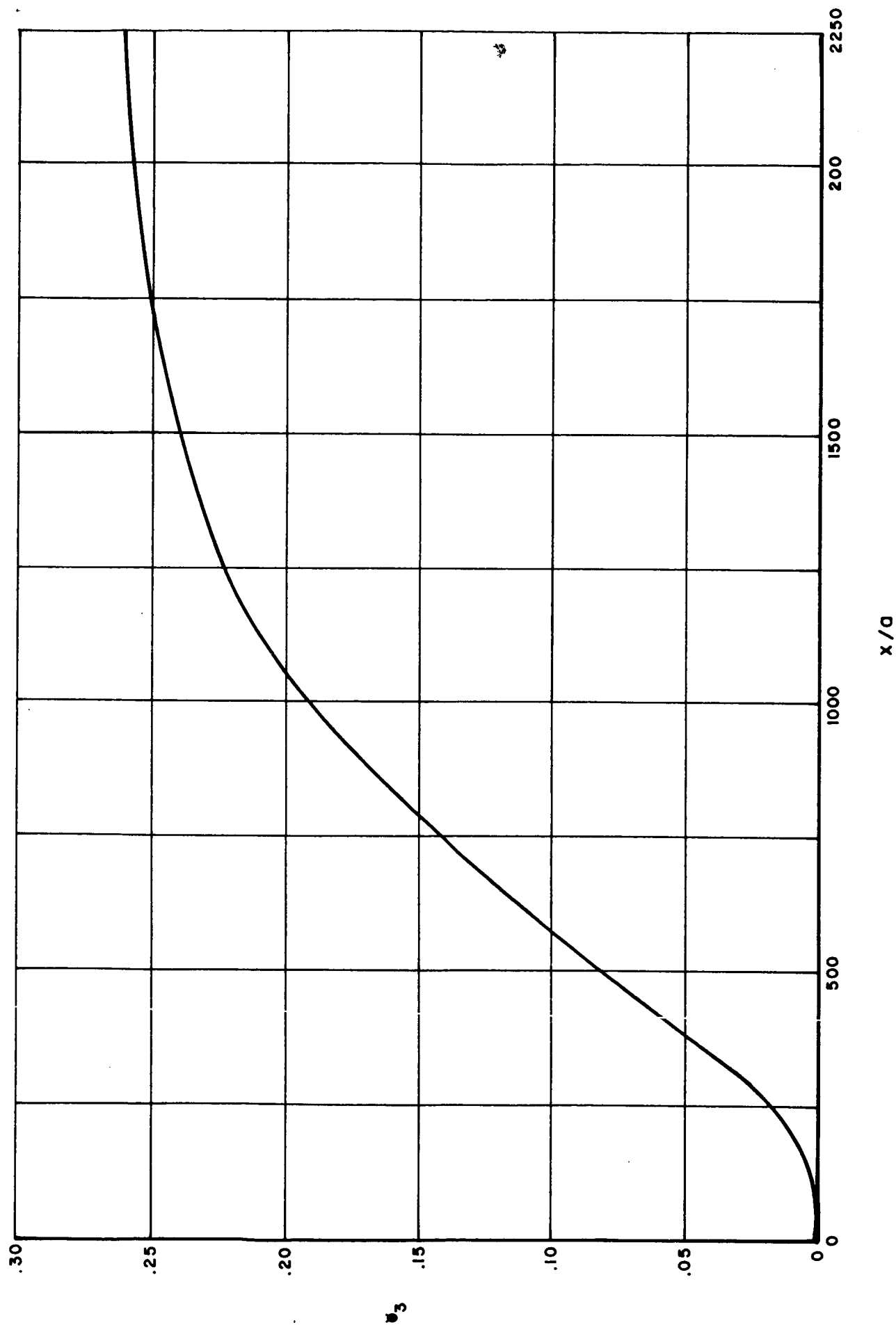
FIG. 16 DISTRIBUTION OF H_2O ALONG JET CENTERLINE LAMINAR T_j = 60 °K
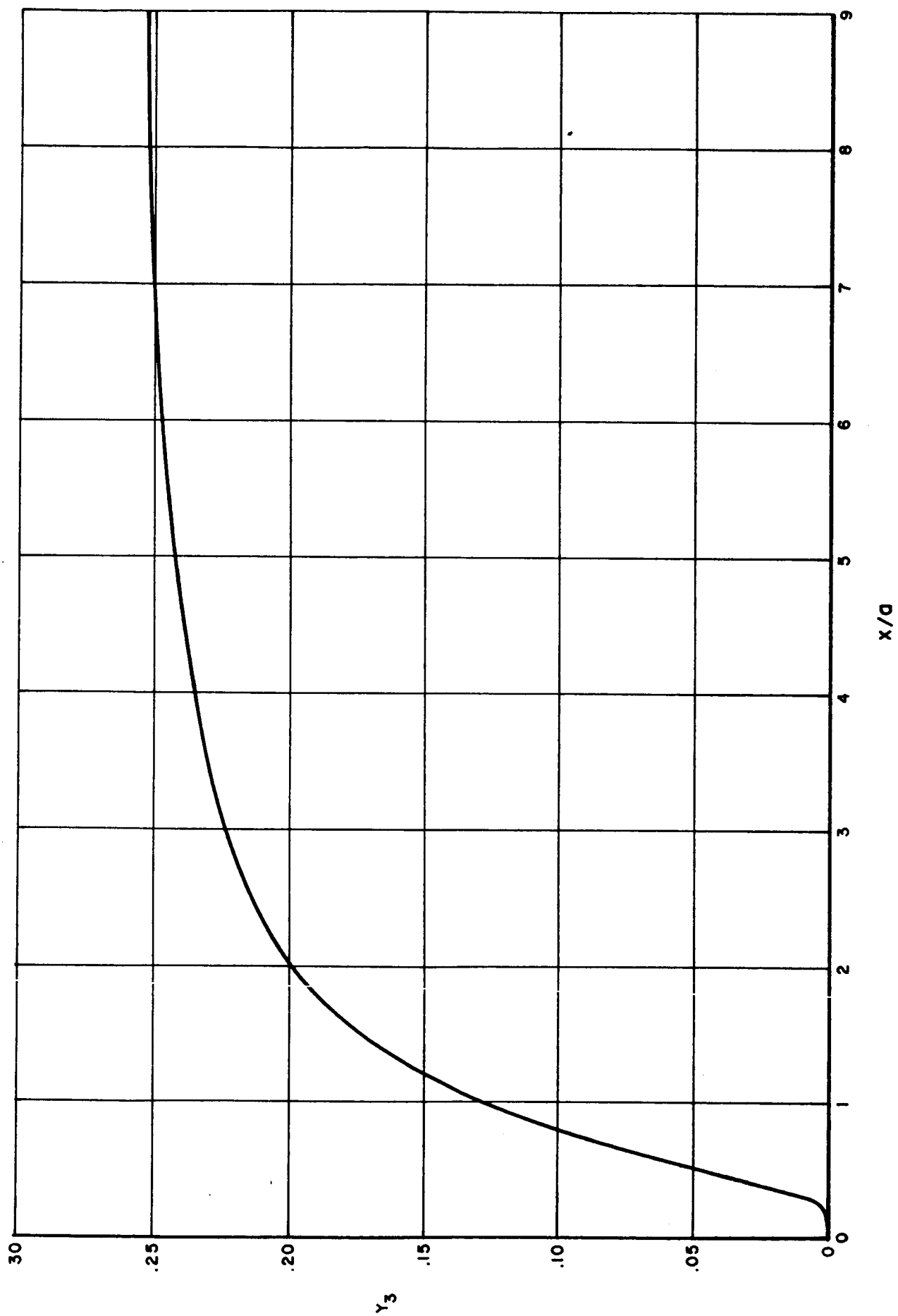
FIG. 17 DISTRIBUTION OF H_2O ALONG THE JET CENTERLINE TURBULENT $T_j = 60\,°K$
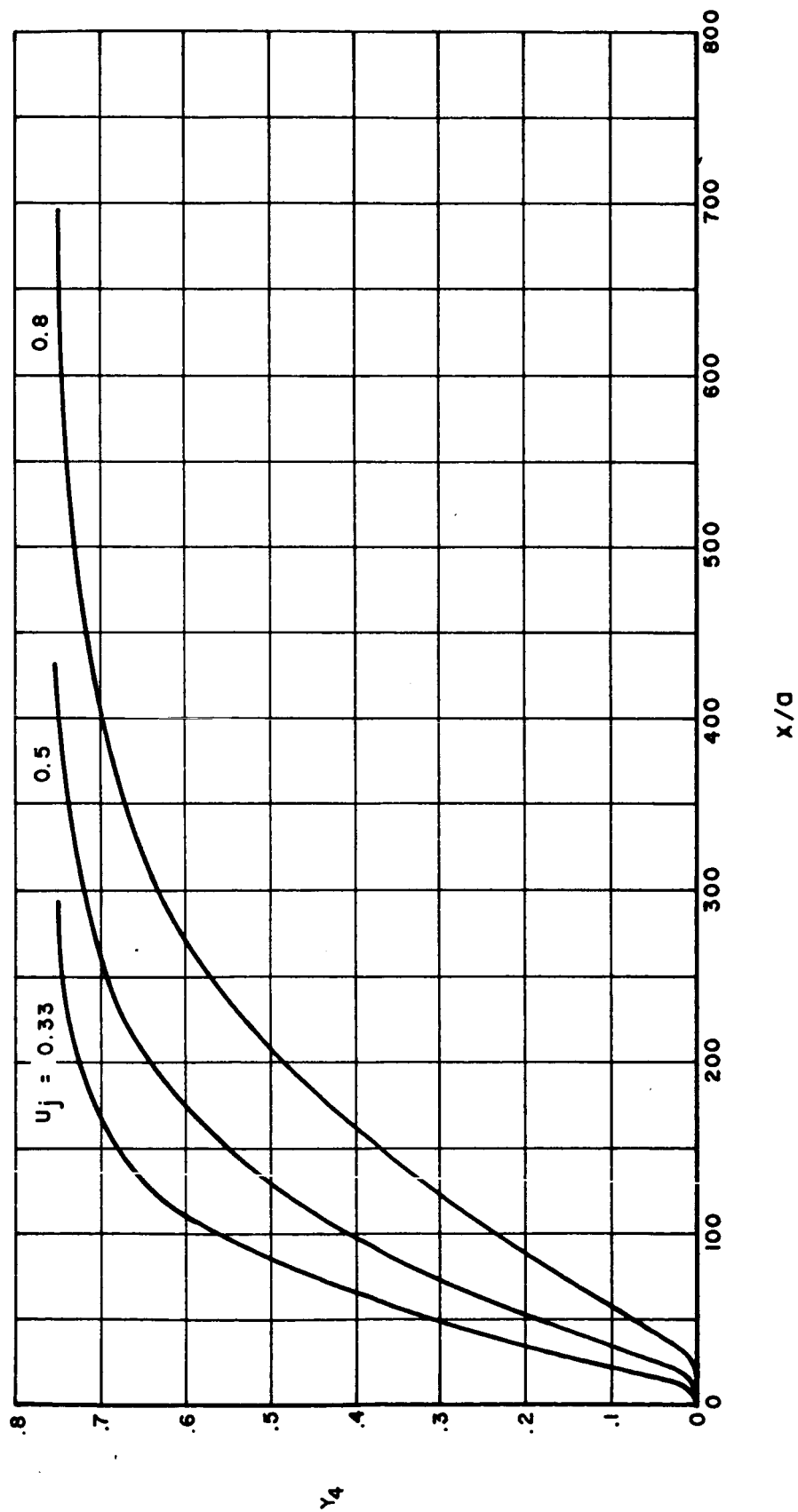
FIG. 18 DISTRIBUTION OF NITROGEN ALONG THE JET CENTERLINE LAMINAR $T_j = 265$ °K
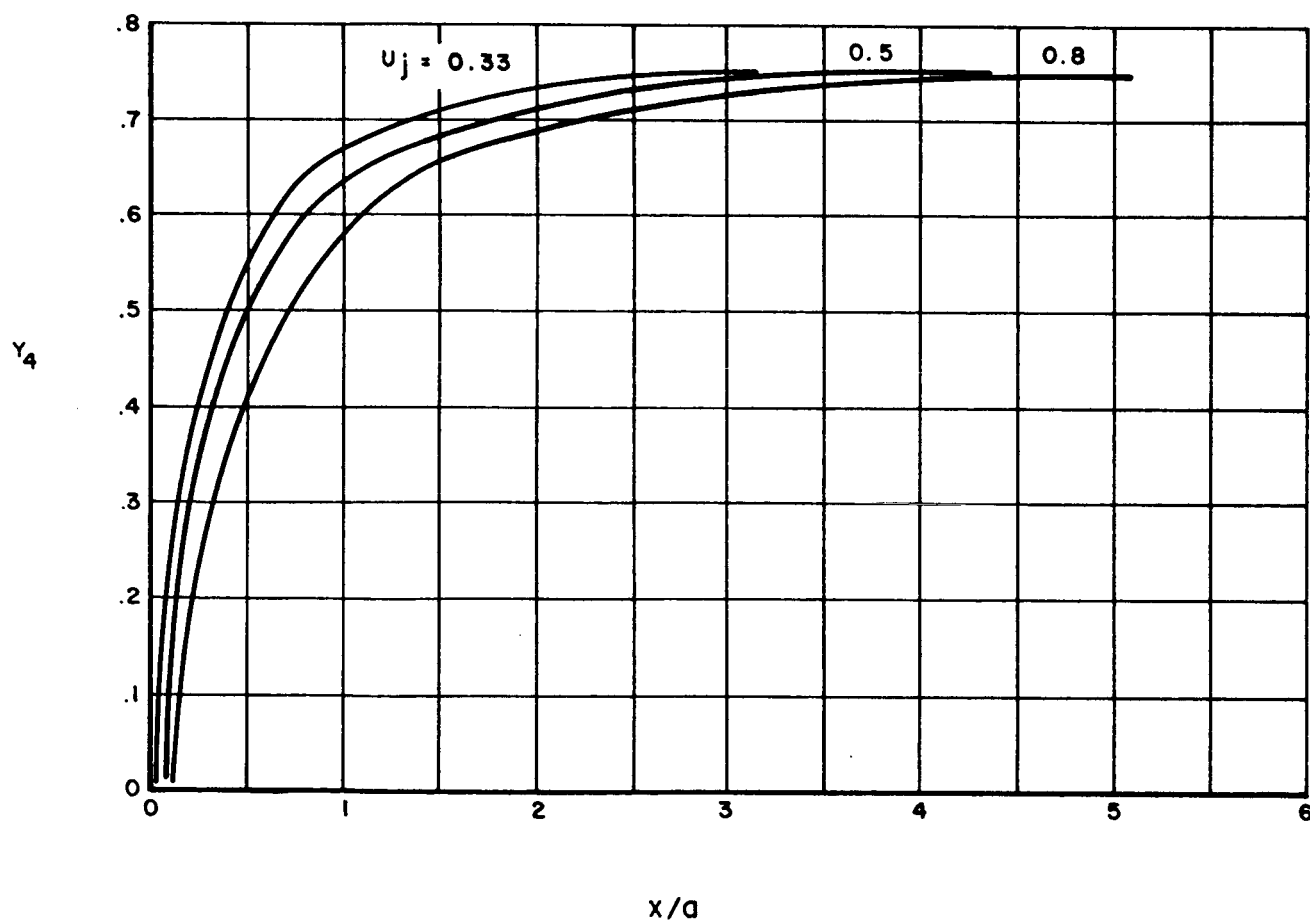
FIG. 19 DISTRIBUTION OF NITROGEN ALONG THE JET CENTERLINE TURBULENT
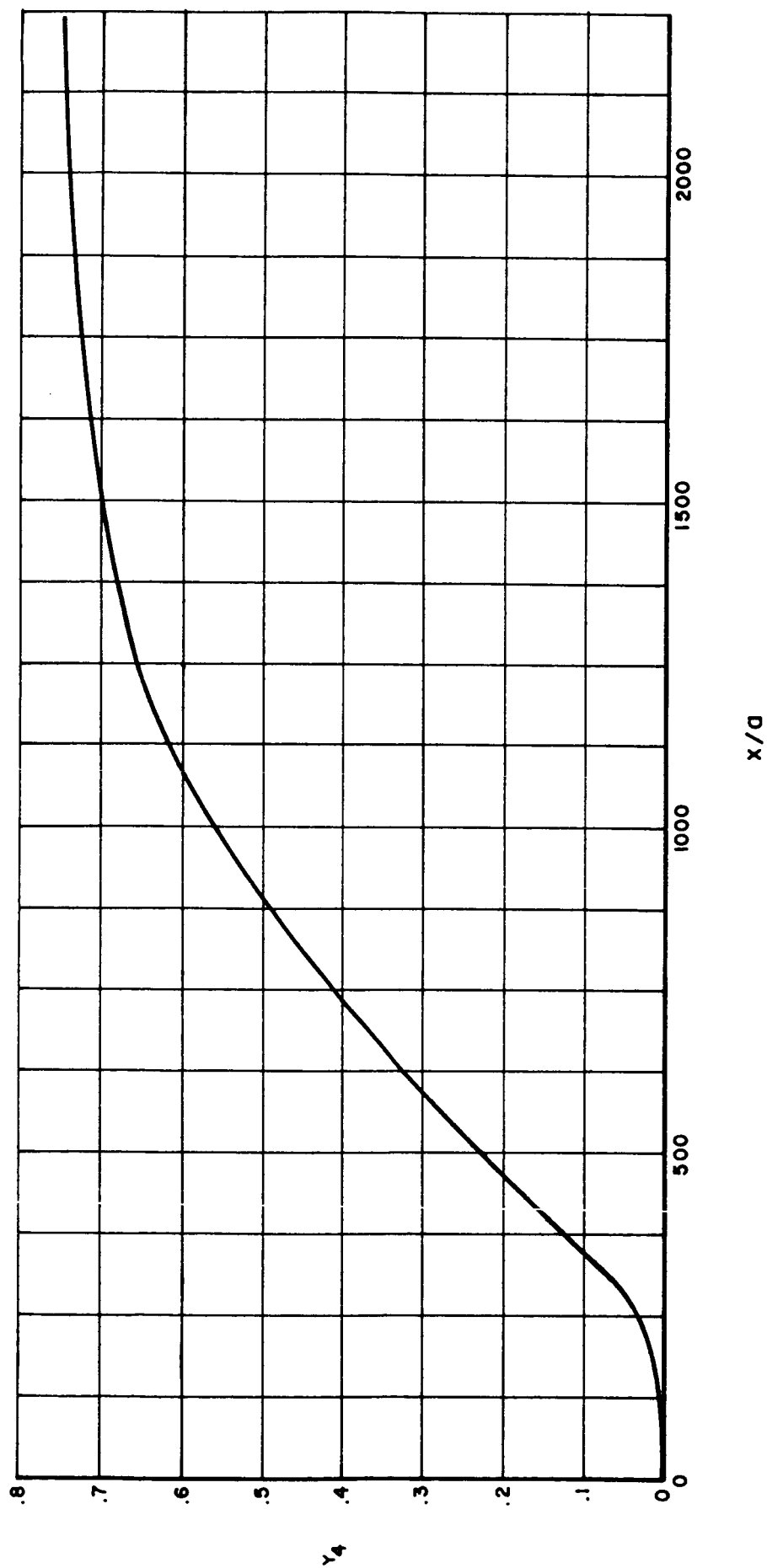
$T_j = 265\ ^\circ K$

FIG. 20   DISTRIBUTION   OF   NITROGEN   ALONG   THE   JET   CENTERLINE   LAMINAR T_j = 60 °K
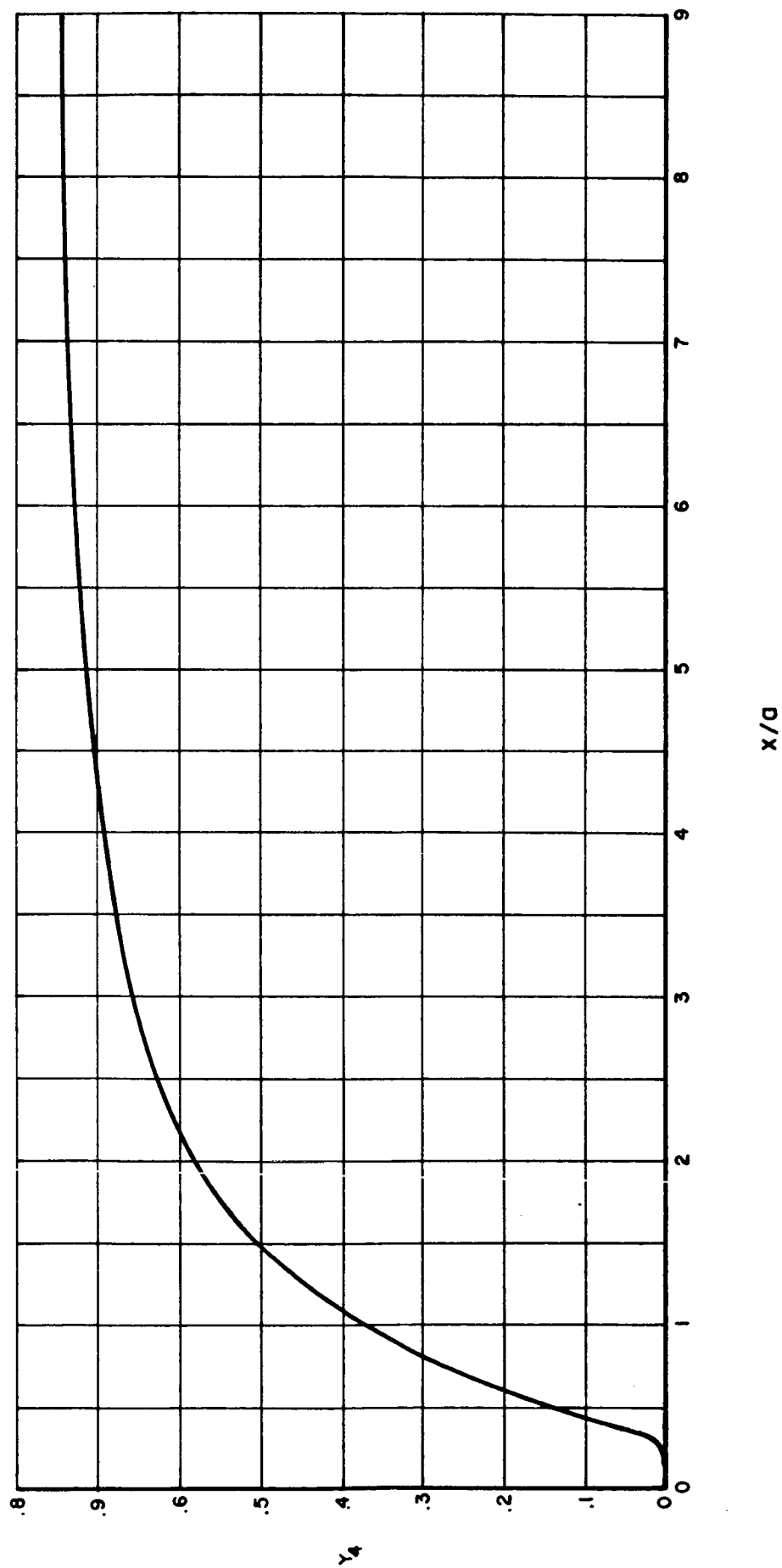
FIG. 21 DISTRIBUTION OF NITROGEN ALONG THE JET CENTERLINE TURBULENT $T_j = 60\ ^\circ K$

40
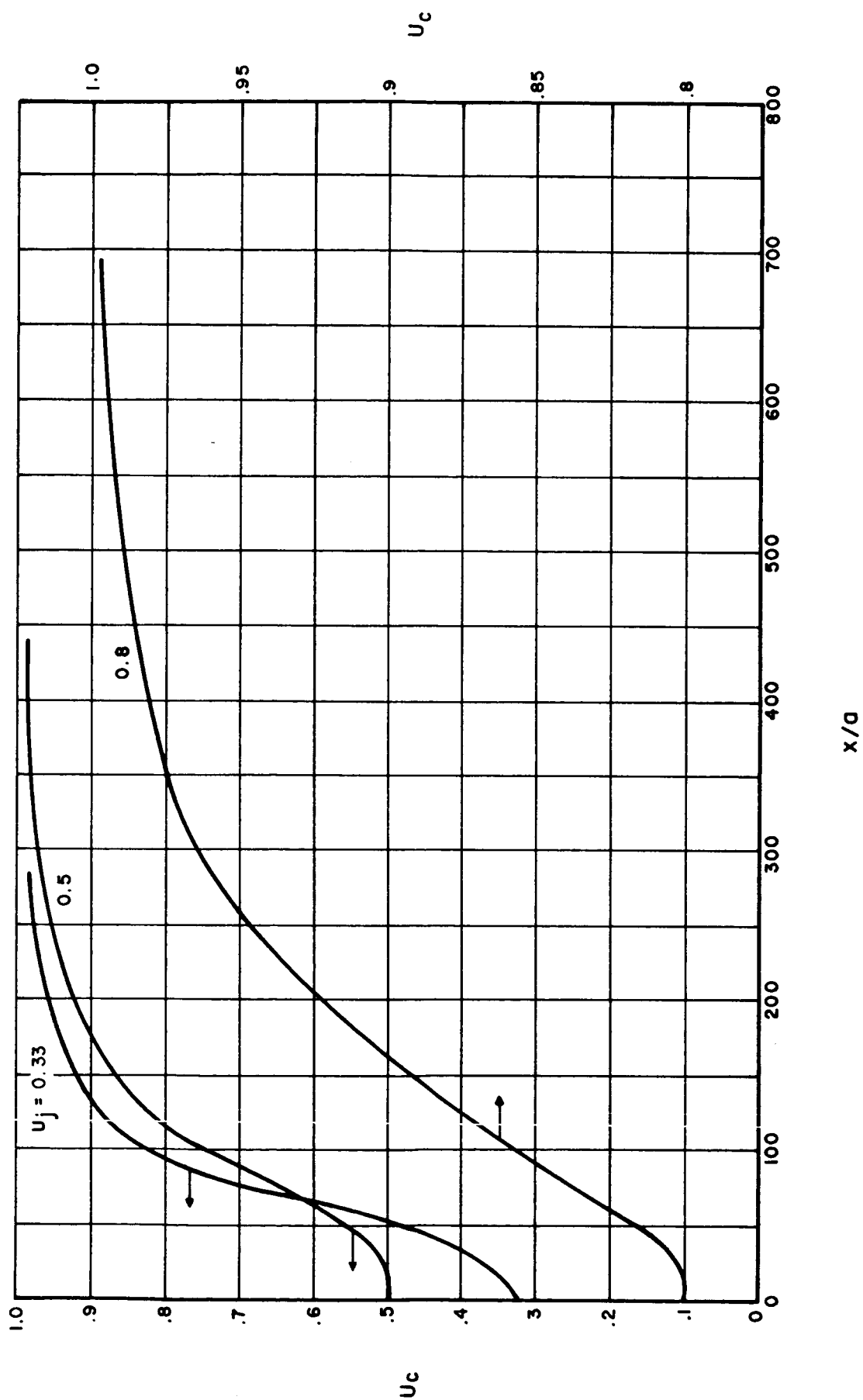
FIG. 22 VELOCITY DISTRIBUTION ALONG THE JET CENTERLINE LAMINAR T_j = 265 °K
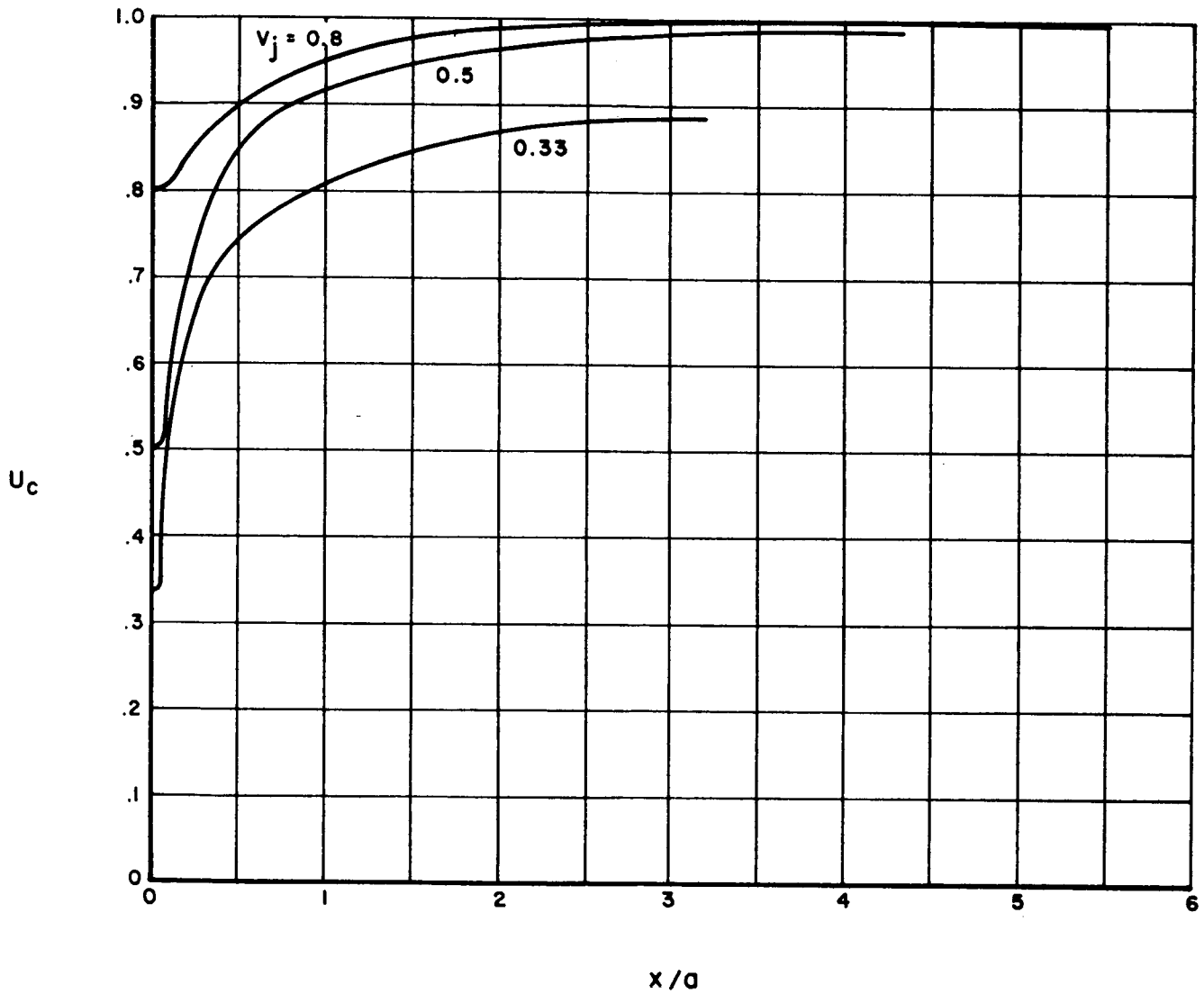
FIG. 23 VELOCITY DISTRIBUTION ALONG THE JET CENTERLINE TURBULENT
T_j = 265 °K
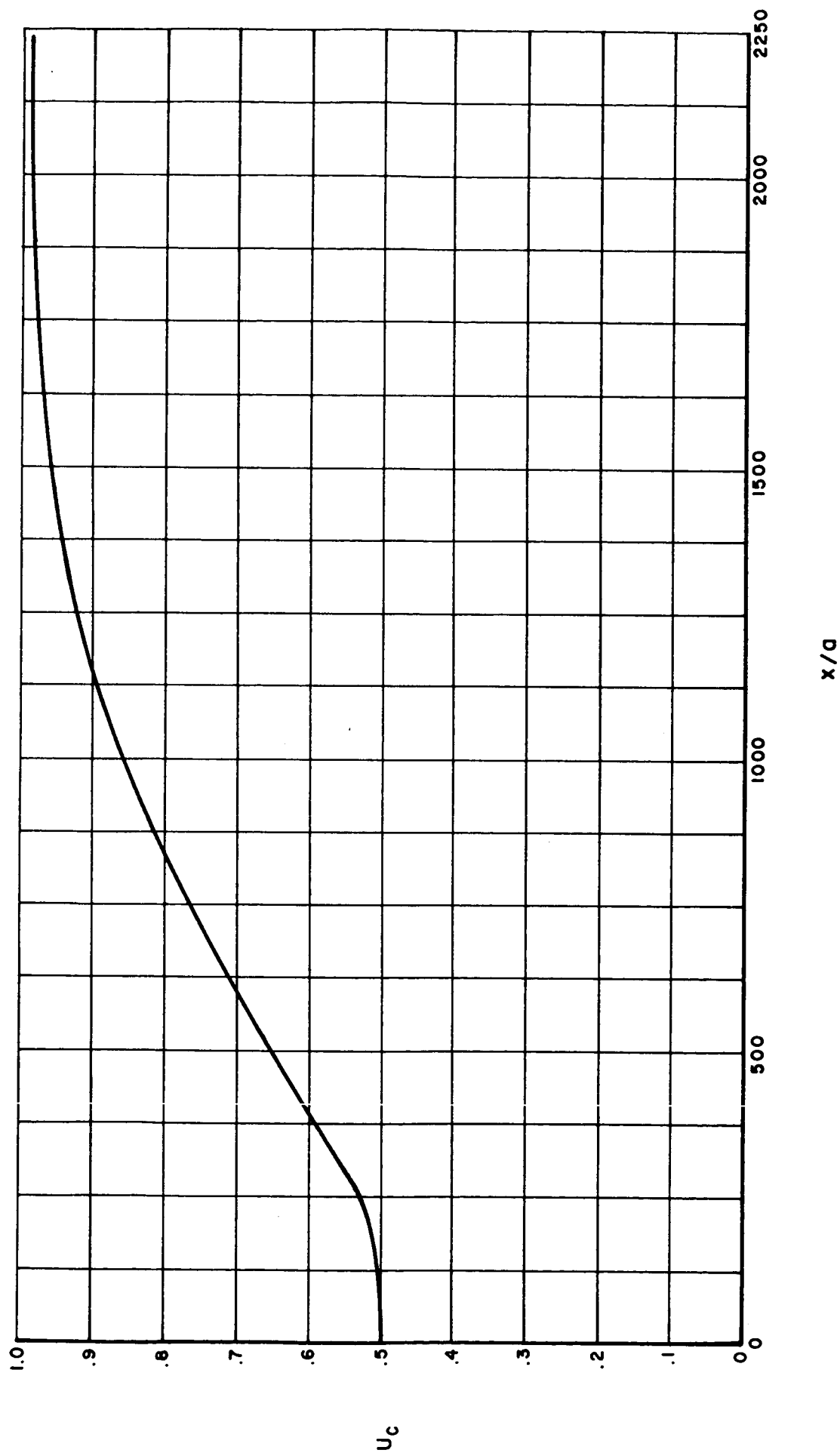
FIG. 24 VELOCITY DISTRIBUTION ALONG THE JET CENTERLINE LAMINAR $T_j = 60$ °K

43
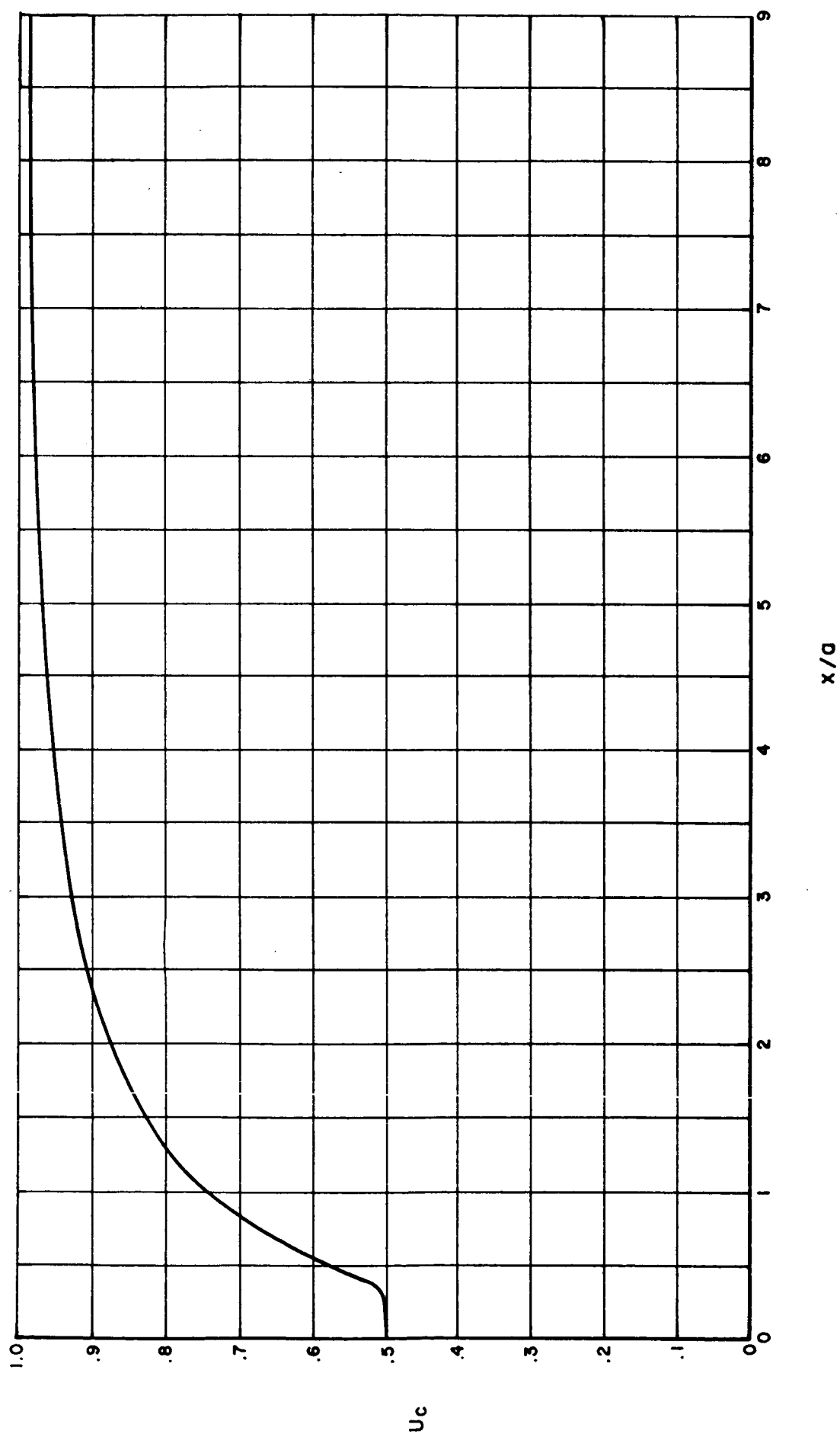
FIG. 25 VELOCITY DISTRIBUTION ALONG THE JET CENTERLINE TURBULENT $T_j = 60$ °K
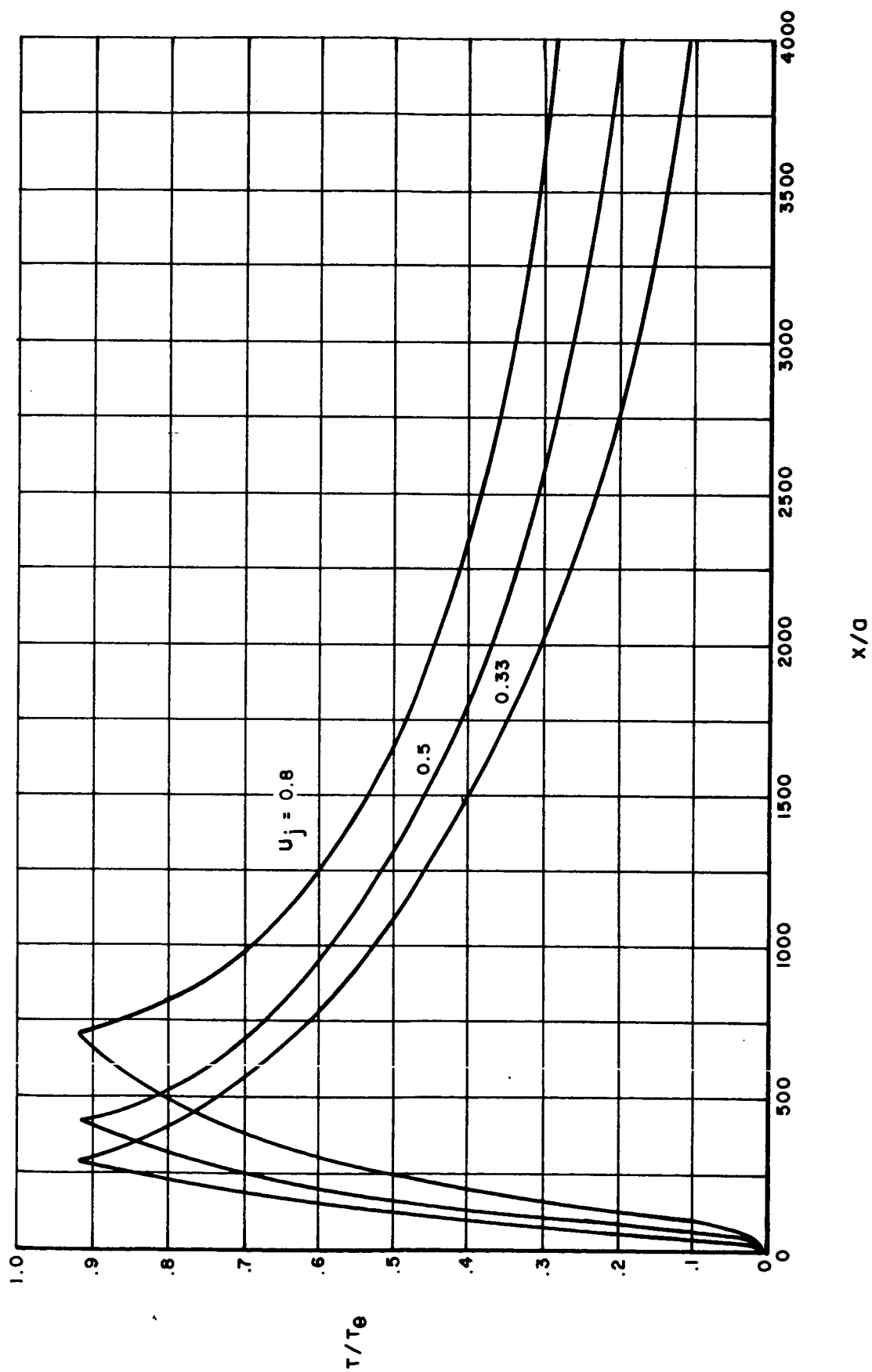
FIG. 26 TEMPERATURE DECAY ALONG THE JET CENTERLINE LAMINAR $T_j = 265$ °K
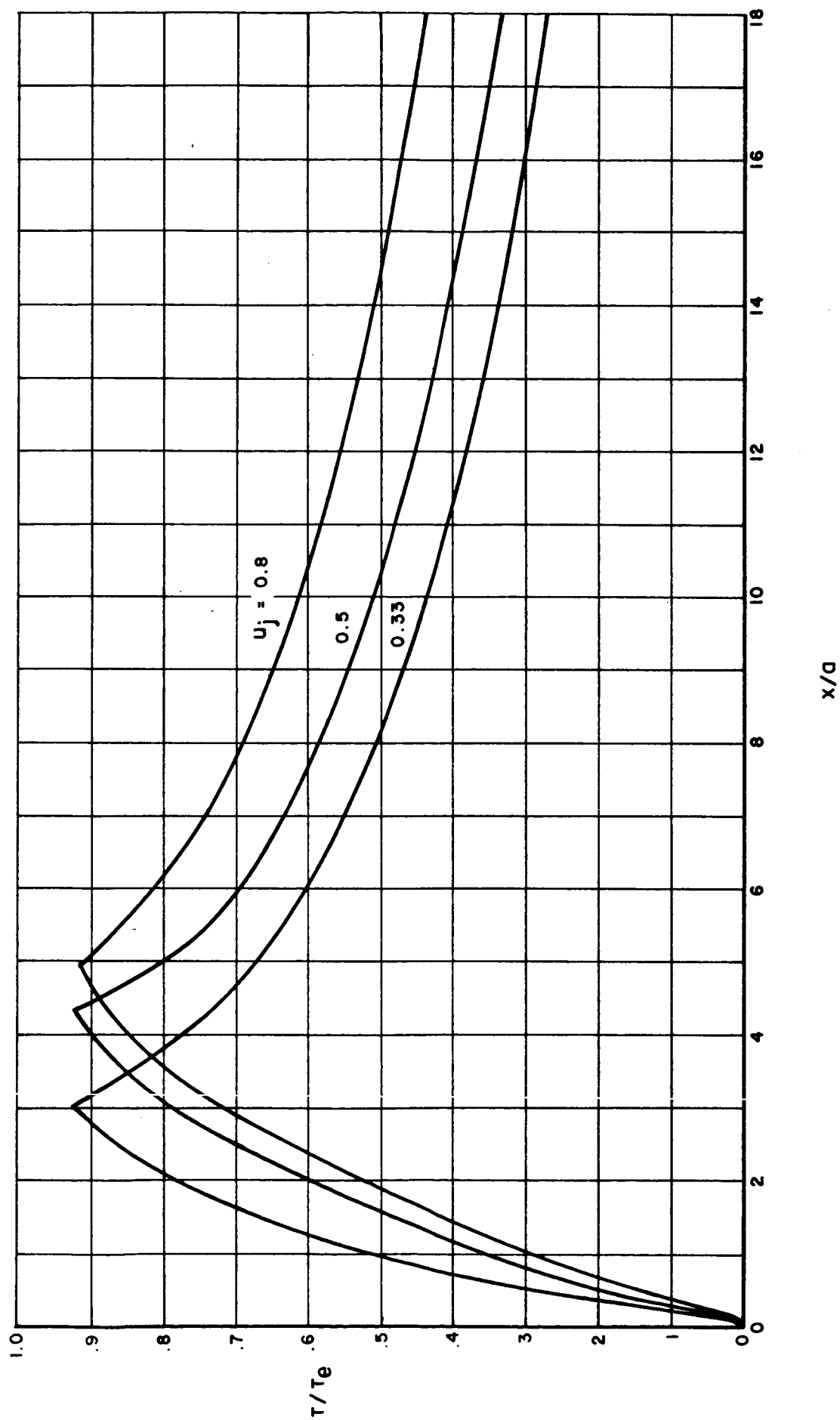
FIG. 27 TEMPERATURE DECAY ALONG THE JET CENTERLINE TURBULENT $T_j = 265 \, °K$

45
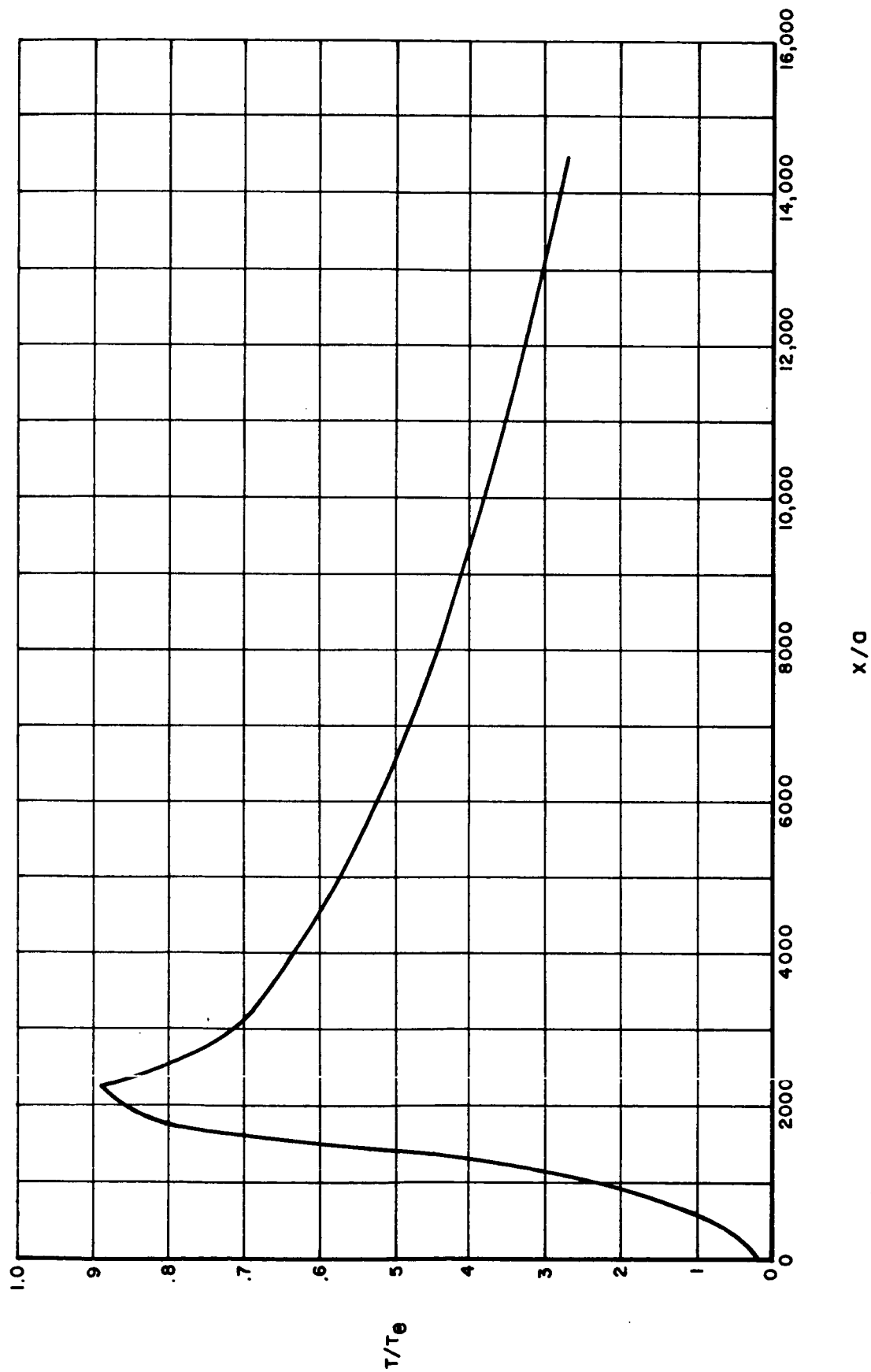
FIG. 28   TEMPERATURE   DECAY   ALONG   THE   JET   CENTERLINE   LAMINAR $T_j = 60\ °K$

47
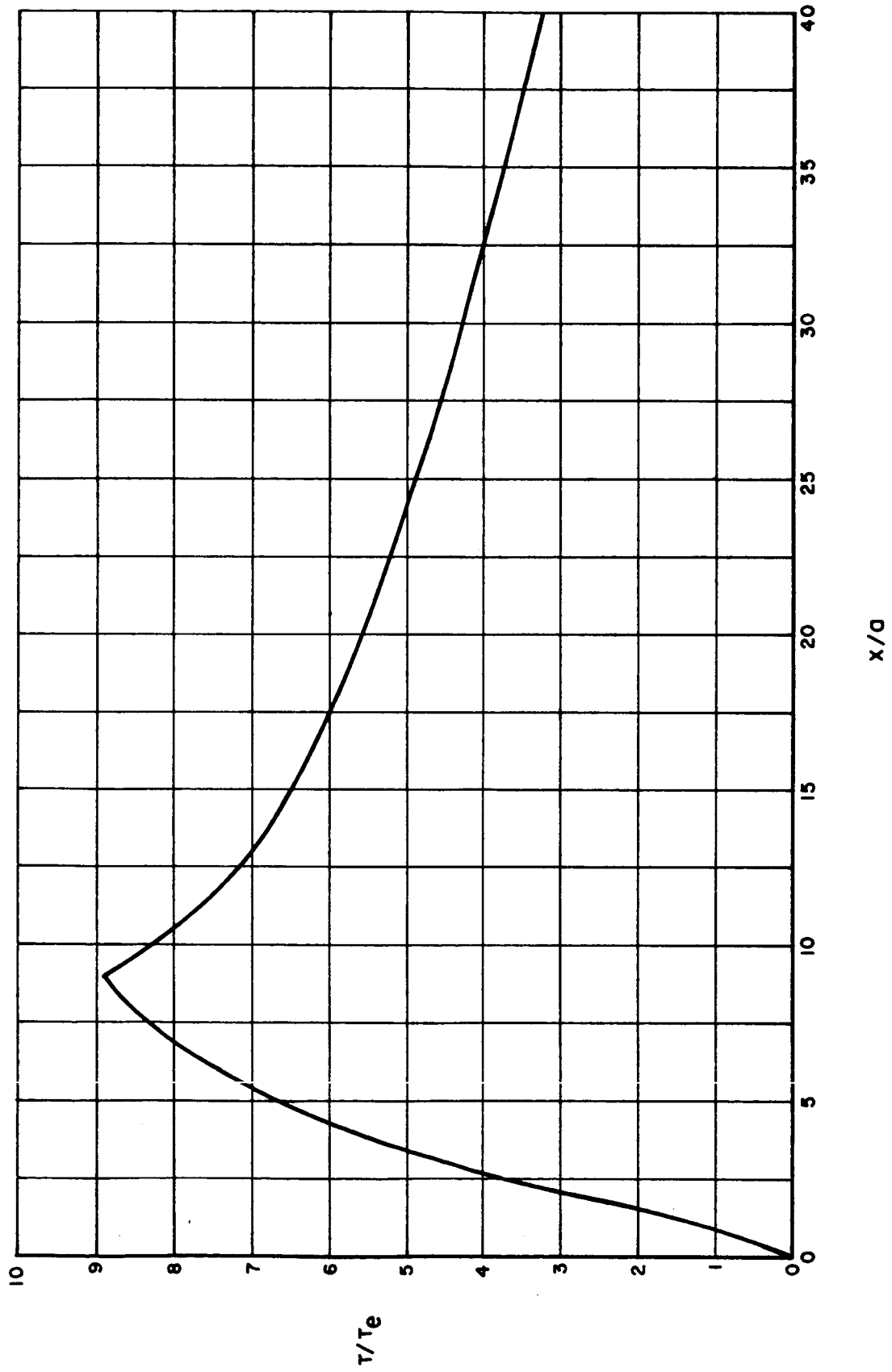
FIG. 29 TEMPERATURE DECAY ALONG THE JET CENTERLINE TURBULENT $T_j = 60 °K$
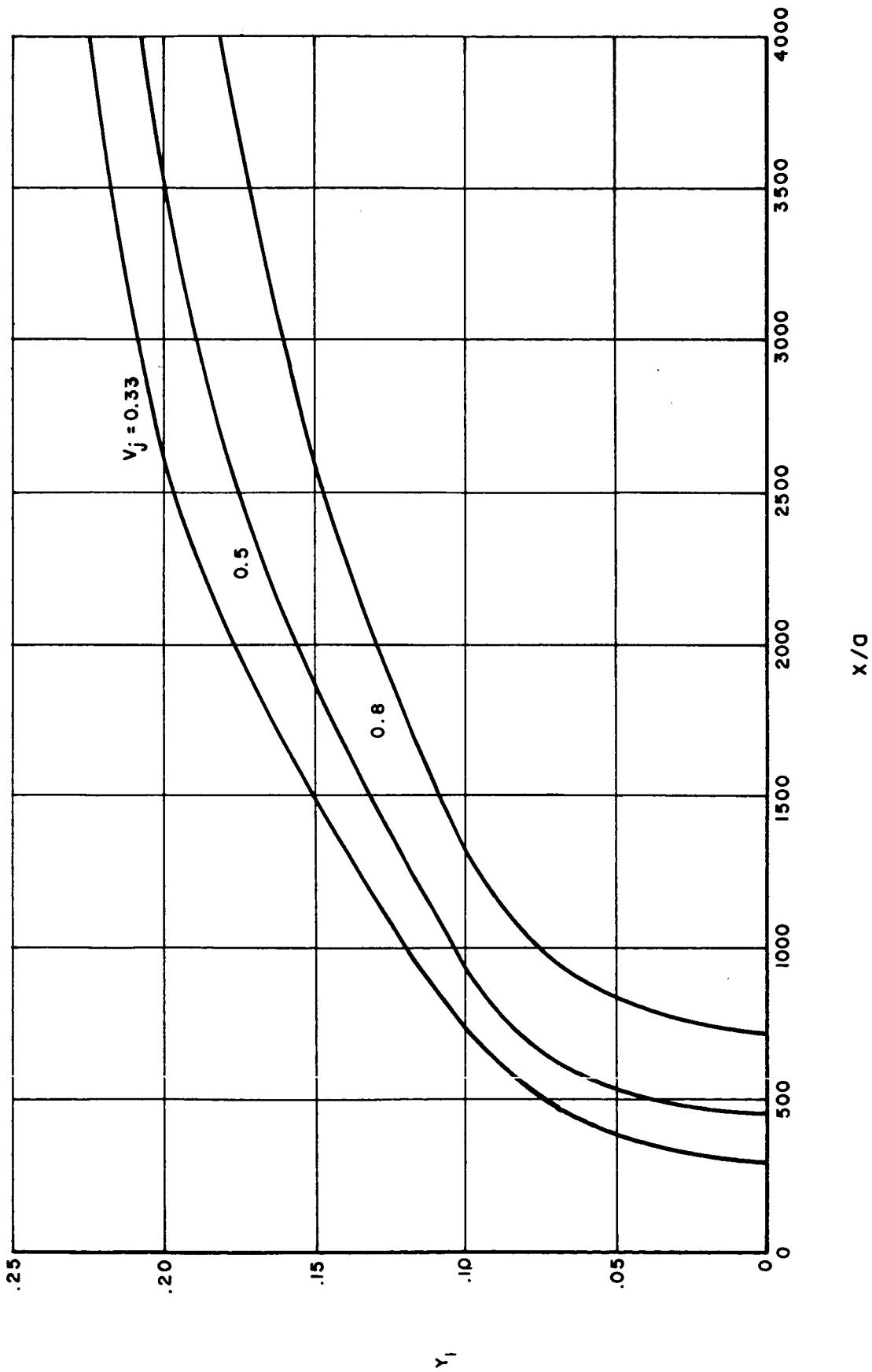
FIG. 30 INCREASE OF OXYGEN CONCENTRATION ALONG JET CENTERLINE LAMINAR $T_j = 265\ °K$
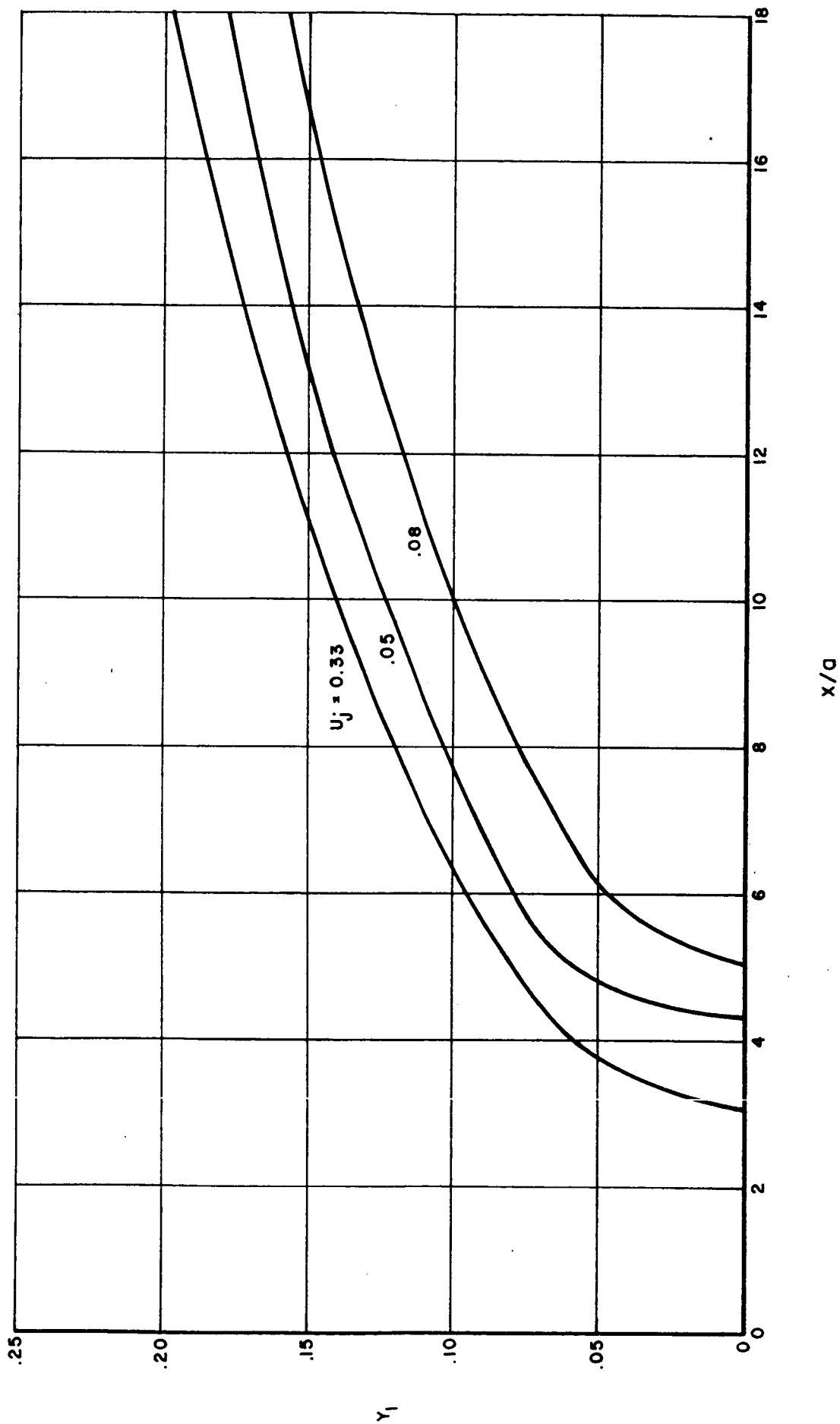
FIG. 31 INCREASE OF OXYGEN CONCENTRATION ALONG THE JET CENTERLINE TURBULENT T_j = 265 °K
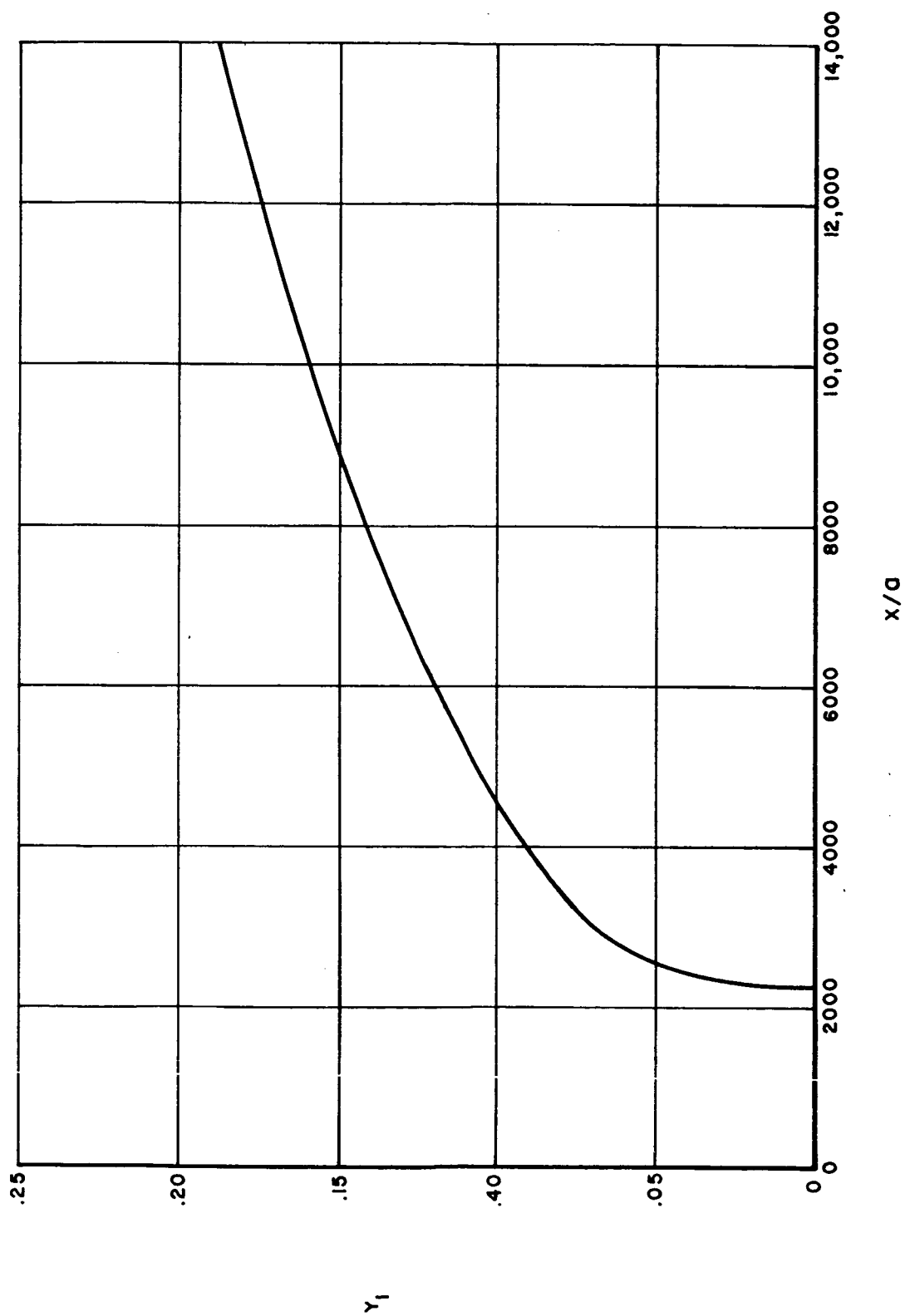
FIG. 32 INCREASE OF OXYGEN CONCENTRATION ALONG THE JET CENTERLINE LAMINAR
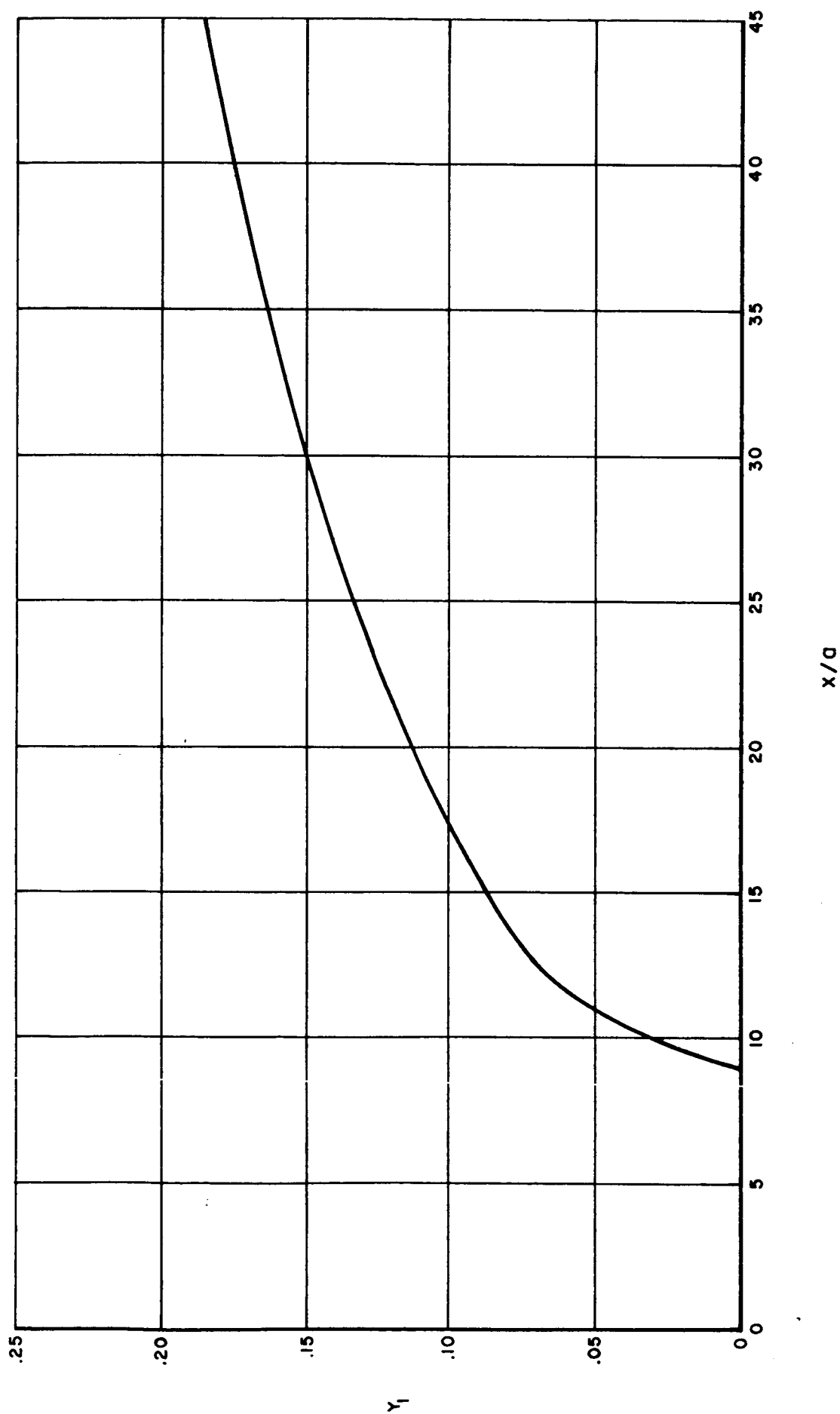
$T_j = 60 \, ^\circ K$

FIG. 33 INCREASE OF OXYGEN CONCENTRATION ALONG THE JET CENTERLINE TURBULENT
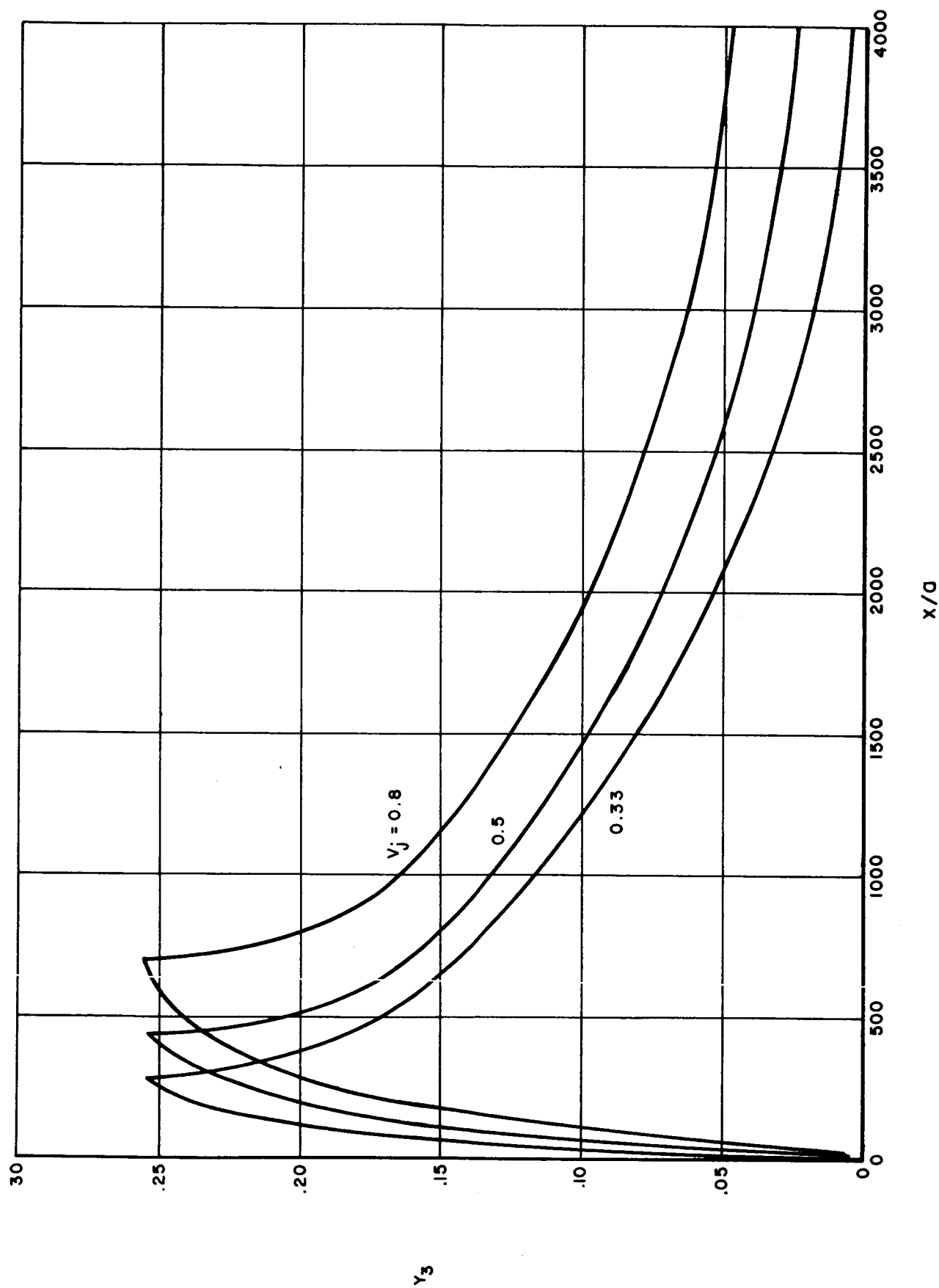
$T_j = 60 \ ^\circ K$

FIG. 34 DECAY OF H_2O CONCENTRATION ALONG THE JET CENTERLINE LAMINAR $T_j = 265$ °K

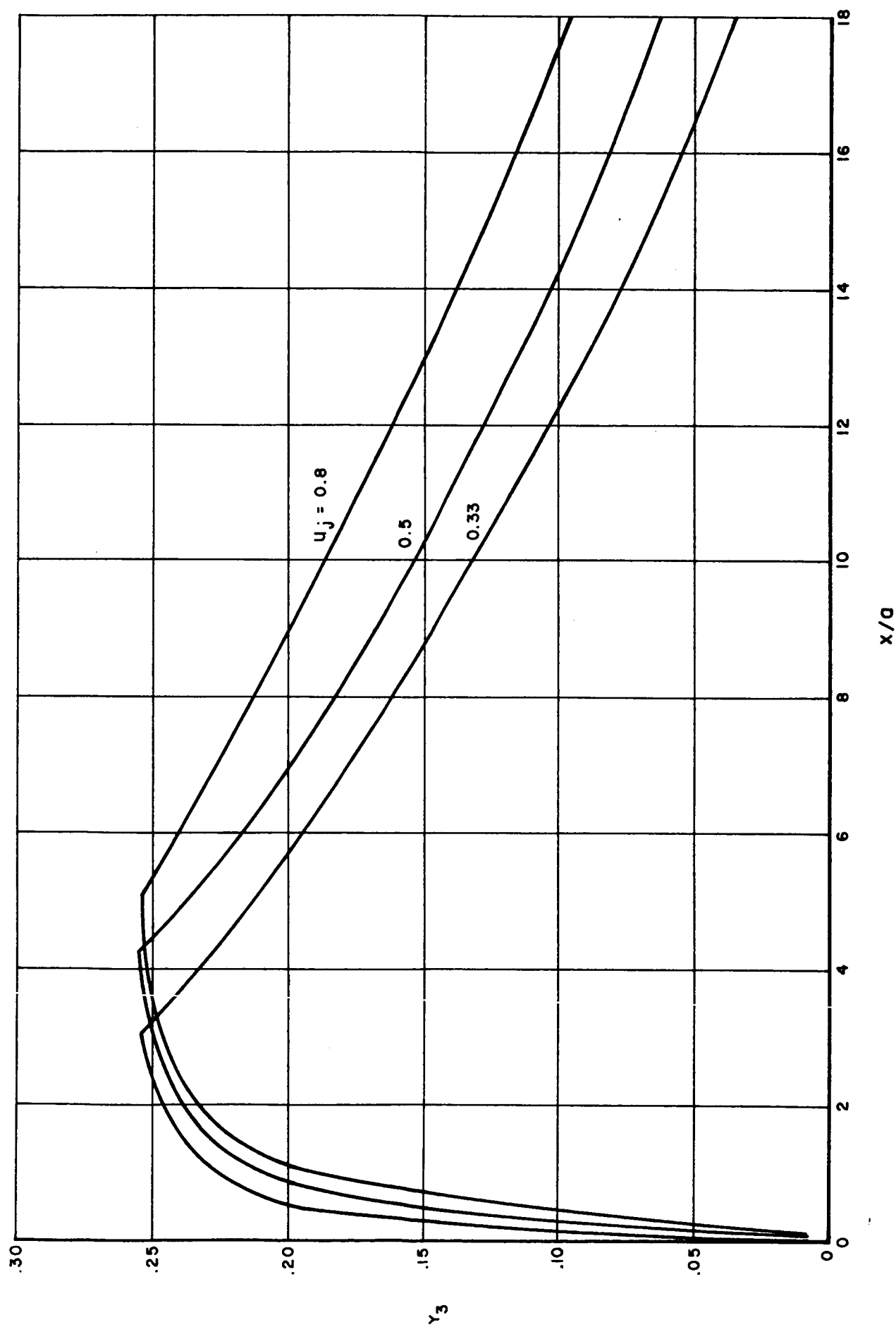FIG. 35 DECAY OF H_2O CONCENTRATION ALONG THE JET CENTERLINE TURBULENT $T_j = 265$ °K

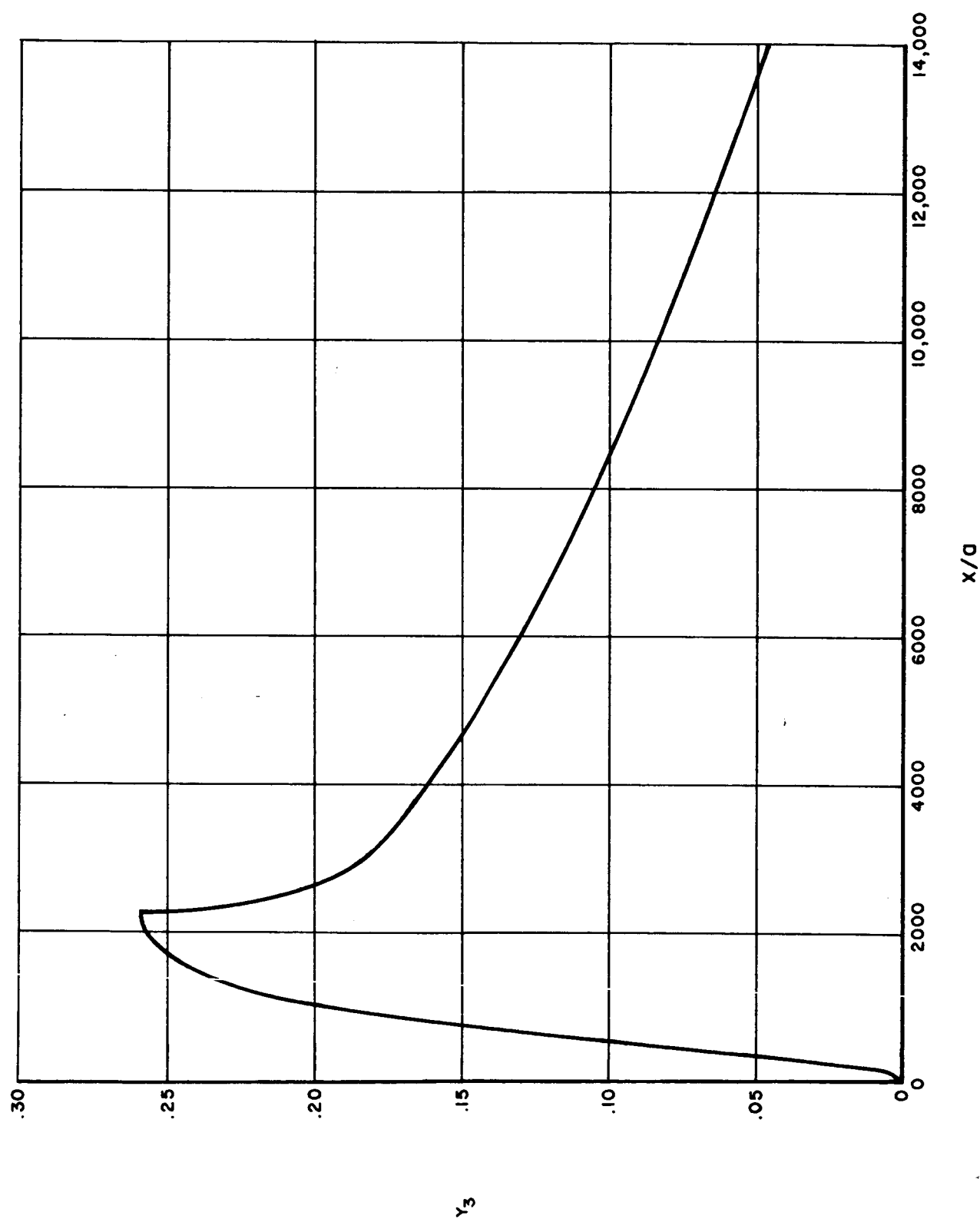FIG. 36 DECAY OF H_2O CONCENTRATION ALONG THE JET CENTERLINE LAMINAR $T_j = 60 \, °K$
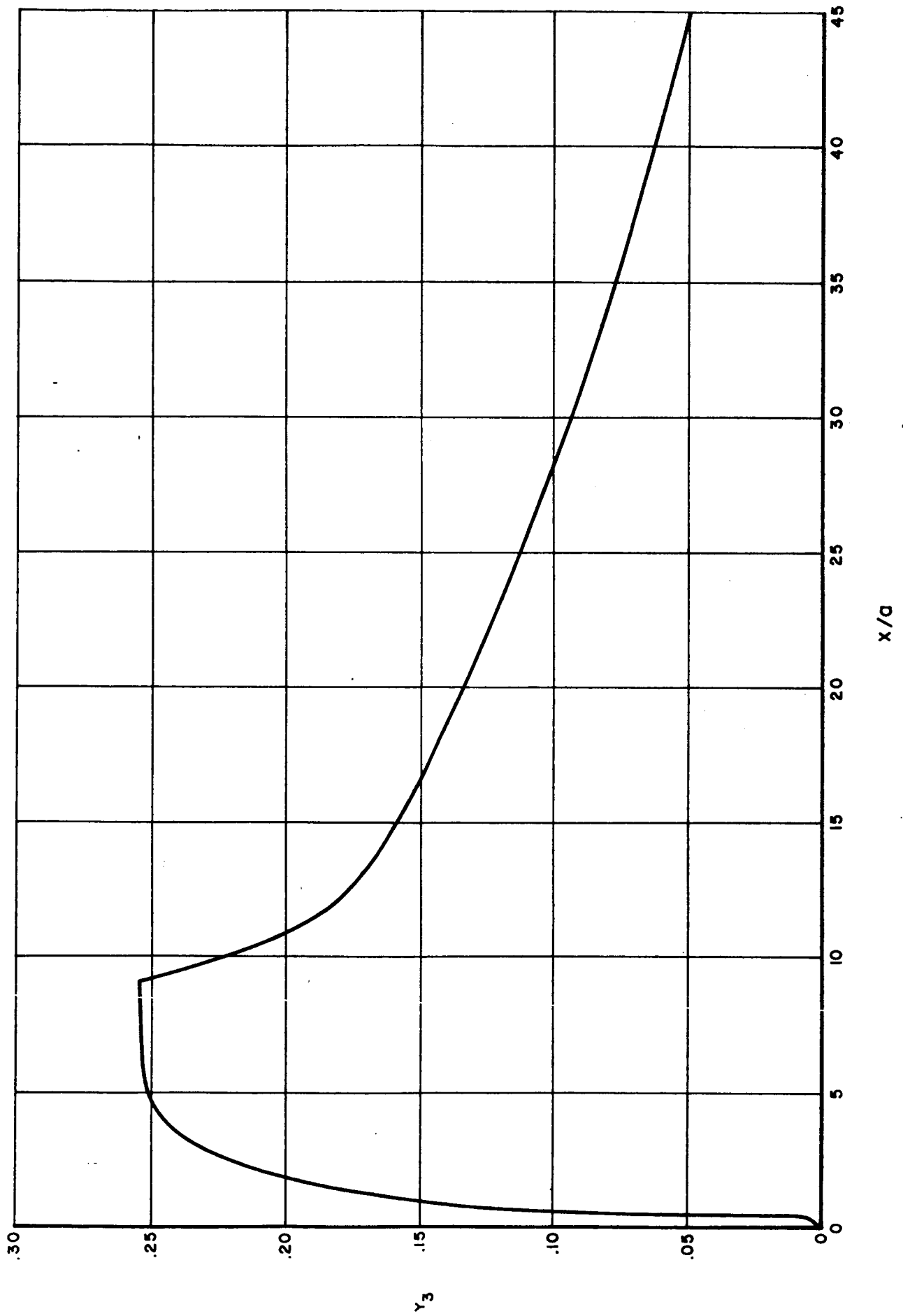
FIG. 37 DECAY OF H_2O CONCENTRATION ALONG THE JET CENTERLINE TURBULENT $T_j = 60 \, °K$